遠洋水研報 第21号 昭和59年2月
Bull. Far Seas Fish. Res. Lab., No. 21, Mar. 1984.

Image analysis of the NIMBUS-CZCS data in the waters adjacent to Japan

Ichiro YAMANAKA*, Tsukasa HOSOMURA,**
and Etsuji KOZASA***

Abstract

A study estimating marine biological productivity by means of NIMBUS-CZCS data was made within the framework of Japan-U.S.A. Cooperative Study Programme.

Among data supplied by NASA were selected two scenes, south of Honshu, Jan. 26, 1979 and west of Kyushu, July 20, 1981. Both imageries were processed by monoband, quasi-real colour and biband false color pictures respectively. Sea truth data were selected from the KER (Kuroshio Exploitation Experiment Research) data.

The absolute values of the correlation coefficient between the logarithm of *in situ* concentration of chlorophyll *a*† or the sum of it and phaeopigment and the logarithm of the ratio of the radiance of the Band 1 (440 nm) and Band 2 (520 nm) or Band 3 (550 nm) were as high as above 0.8.

The correlation between the pigment concentration and the ratio of the radiance of the Band 1 and the sum of that of Band 1 through Band 5 (both in logarithm) was shown also high.

The oceanographic boundary shown in the biband picture was shown conformed to that shown in the distribution of temperature, salinity, and chlorophyll *a* (plus phaeopigments) obtained by vessels data.

A trial to remove the path radiance was also made. The result however, did not much affect the estimation of chlorophyll distribution.

(Note† Unless specially notifed, "chrolophyll" measured by CZCS means "chrolophyll *a* ".)

Received Dec. 1, 1983. Contribution No. 229 from the Far Seas Fisheries Research Laboratory.
Received Dec. 24, 1983, Contribution No. 414 from the Seikai Regional Fisheries Research Laboratory.

* Far Seas Fisheries Research Laboratory, 5-7-1 Orido, Shimizu 424, Japan : present, Japan Fisheries Information Service Center, 1-7, Kojimachi, Chiyoda-ku, Tokyo 102 Japan.
** Tokai University Research and Information Center, 2-28, Tomigaya, Shibuya, Tokyo 151, Japan.
*** Seikai Regional Fisheries Research Laboratory, 49 Kokubucho, Nagasaki 850, Japan.

Contents

Preface

For the study of fisheries oceanography, the information of sea color is no less important than that of abiotic environmental parameters such as temperature and salinity, because it is closely linked to biological productivity of the ocean. However, the accumulation of synoptic data on biological productivity is rather poor at present mainly partly due to the limitation of research cruises.

As to the application of remote sensing method of photometry of ocean color, the multiple spectro-scanner (MSS) equipped aboard the aircraft has been proved rather successful (e. g. Hovis and Leung, 1977). The MSS of LANDSAT were also tried to find fishing ground. (e. g. Kemmerer and Buttler, 1977). The latter is however still not satisfactory for several weekpoints as described in the next section.

The Coastal Zone Colour Scanner (CZCS) aboard the satellite NIMBUS-7 launched by NASA in the autumn of 1978 had been expected to play an important role in the field of biological oceanography and fisheries, because of its spectrometric specification, (e. g. Watanabe 1977 etc.).

A research project to analyse the CZCS data for studying marine biological resources was initiated as one of the Joint Research Programmes with a cooporation of Japan and U. S.

The present report describes the results obtained by 1982 and discusses about the outstanding problems to be solved in the future study.

I. Features of CZCS data compared to those of LANDSAT for marine biology

In spite of their successful uses of the LANDSAT data in many fields, they have the following defects in marine biologcal study.

(a) The area covered by one scene (185 km × 185 km) is wide enough only for the research of limitted coastal area, but inadequate for the study of open sea area.

(b) The time interval of 18 days for its returning is too long for the continuous monitoring of sea colour in an area particularly if the weather conditions hinder the area frequntly.

(c) The band width of each channel of LANDSAT (100 nm each) is too wide for the chlorophyll measurement. As is shown in the Fig. 1 (Ramsey, 1963, calculated after the Hulbert's (1943) equation), the Band 4 of the LANDSAT-MSS (500-600 nm), for example, covers various level of reflectance and averages it up for a certain chrolophyll concentration. Accordingly the sensibility of the averaged reflectance is impaired for the chlorophyll concentration measurement.

(d) The 440 nm band which plays an important role in chlorophyll measurement, particularly for low concentration because of the strong and negative correlation to the chlorophyll concentration is lacking in LANDSAT.

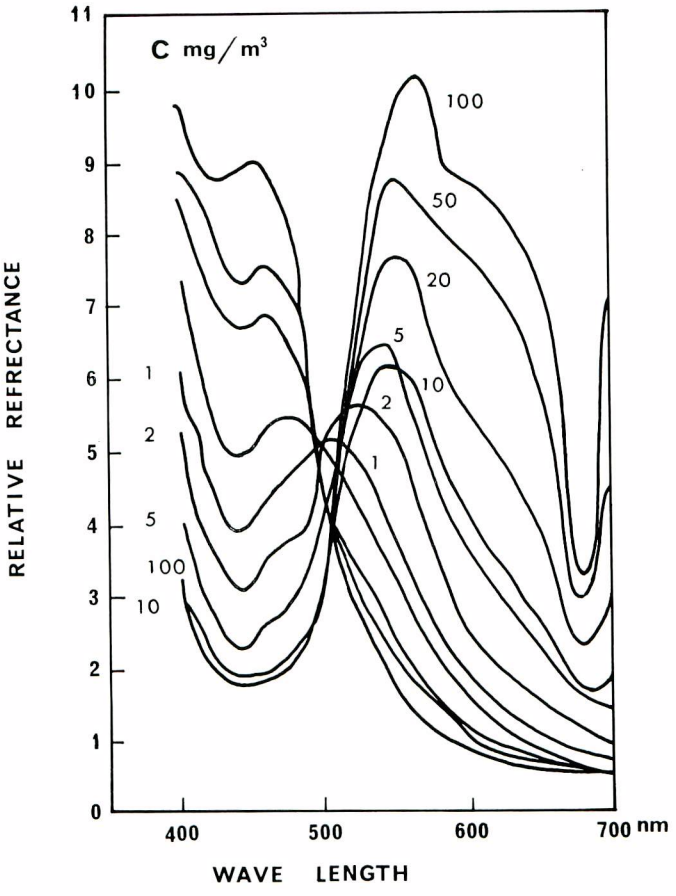

Fig. 1. Spectral reflectance at various concentration of the chlorophyll (after Ramsey 1968)

(e) In most case the radiance scale obtained from LANDSAT is too monotonous on the sea. The gain level of the reception has to be elevated in order to enhance the information of the sea. This process, however, inevitably cuts off the land information.

The CZCS was devised with careful attention for the purpose of chlorophyll measurement in open ocean notwithstanding its name. The size of each pixel is 825 m × 825 m, much coarser than LANDSAT's 80 m × 80 m, meanwhile the area covered by a scene is as wide as 1,566 km × 700 km ; and three sequential scenes are usually included in a reel of data tape.

Therefore the total area of an image can cover whole waters around Japan if the weather is fine. The time interval of its returning is six days, much shorter than that of LANDSAT. Therefore if we do not care whether the target area is pictured in the center or the fringe of the image, we can expect to obtain the information almost every day unless the obstacle of the cloud.

The spectrum band is as narrow as 20 nm for the vissible wavelength. Besides it has

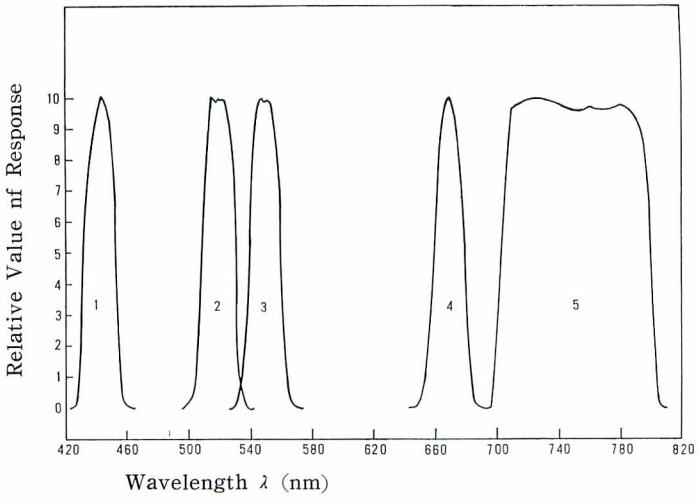

Fig. 2. CZCS Spectral response for bands 1 through 5

a near infrared and a far infrared bands (Fig. 2).

The Band 1 (440 nm) sharply responds to the chlorophyll concentration for low value of it. The concentration negatively correlates to the reflectance. A minimum of reflectance is seen for all values of the concentration at 440 nm.

The Band 2 (520 nm) is so-called the hinge point at which the reflectance does not respond to the chlorophyll concentration.

The Band 3 (550 nm) responds to the chlorophyll concetration as an inverse manner to the Band 1 ; namely the reflectance positively correlates to the concentration. There is a maximum of reflectance at 550 nm for all value of concentration.

The Band 4 (670 nm) shows minimum of reflectance for all value of concentration. But the correlation between the reflectance and concentration is positive just as the case of the Band 3.

The Band 5 (780 nm) is used for detecting vegetation on the land because of the strong reflection of chlorophyll of land plants. But that from the sea is very weak. Therefore, it is used to know the sea from the land.

The Band 6 (10.5-12.5 nm) is the infrared wave and used to measure the sea surface temperature.

II. Results of preliminary studies

Within the framework of the "Joint Cooperative Programme of Japan and U. S. A. in the Non-Energy Field", it has been agreed that NASA would supply CZCS data for the exchanging of Japanese oceanographic data.

The CZCS data around Japan, however, arrived Japan much behind the original schedule.

In advance to the arrival of the first data around Japan, a reel of Calibrated Radiance Tape (CRT) of the Orbit # 1998 (off Baja California, Mar. 17, 1979) was purchased through the Japan Remote Sensing Technology Center (RESTEC) for the preparatory exercise of data handling. The tape was processed by the Tokai University Research and Information Center (TRIC).

II-1 Software developed by TRIC

The following set of software was devised by TRIC.

(a) Reading out the header-file of the CRT: —— Parameters for identification of the CRT.

(b) Reading out the documentation record: —— Parameters relevant to analysis, such as the date in Julian day, start time of the scan in millisecond, latitude and longitude of the center and corners of the scene, orbit number etc. Parameters relevemt to air correction, (zenith distance and azimuth of the Sun and the view line, tilt angle of the sensor), parameters for converting the radiance count number (0-255) to the radio-metric value (mw/sq. cm-str. μm), and that of the Band 6 to temperature, are also contained.

(c) Reading out the information of location and posture of the sensor —— The data occupy the last part of the documentation file. The position of the satellite, altitude, speed, pitch, roll, and yaw are shown for several times during the flight over the target area.

(d) Sampling of pixels corresponding with the sea truth data —— 25 pixels centered at the vessels observation stations, and the value of maxima, minima, means, standard deviations, and modes of radiance counts were calculated.

(e) Geometric correction —— In CZCS each scanning line is expressed by the latitude and longitude of 77 anchor pixels. By iterative experiment the fifth power curve was found satisfactory to express the curve of a track of the orbit on the earth. (Appendix of this report.) The transfiguration from the original picture to the Mercator's projection was also made.

The software (d) and (e) were made after the CRT data around Japan were delivered.

II-2 Data processing exercise by the data Orbit # 1998

Besides the monochromatic picture of each band, black and white pictures of the ratio, R1/RS, R 3/RS, R 1/R 2, R1/R 3 etc. and a false colour picture of R 1/R 2 were made. Here RI and RS denote the radiance count number of the i-th band and R 1 + R 2 + R 3 + R 4 respectively.

Although it was not possible to discuss the validity of these products because of the lack of effective sea truth data, it was found the picture of R 1/R 2 suggests some hydrographical conditions of the sea ; high concentration of chlorophyll is indicated off the Colorad and the Sacramento Rivers, respectively.

An inverse correlationship is seen in gray scale of R 1/RS and R 3/RS pictures. This fact will be discussed in dealing with the data aroud Japan.

III. Selection of CZCS data around Japan

Several cruises were selected among existing chlorophyll data obtained by the Kuroshio Exploitation Research (KER) programme so as to make them match for the use as the sea truth data to compare with the satellite data.

In the period between March 1980 and June 1981, NASA sent fifteen reels of CRTs (Calibrated Radiance Tape) to Japan on the request of the Far Seas Fisheries Research Laboraory.

The following criteria were adopted to select the data to be analysed among the whole volume of CRTs arrived.

Step 1. Reading out the documentation file : — The latitude and longitude of the corners was checked to select the adequate area for sea truth comparison.

Step 2. Selection by cloud distribution data : — The cloud distribution map compiled by each six hours estimated by the data of the Geostational Meteorological Satellite (GMS) and published by the" Monthly Report of the Japan Meteorological Center" could be used in selecting out suitable cloud free scenes.

Step 3. Quick look selection : — In order to avoid the misclassification due to the time lag between the CZCS and GMS data, a sheet of black and white picture of the Band 3 was prepared for each data selected the criterion Step 2.

Through the three procedures, Orbits #1297 and #8774 were finally chosen for process and for calibration with the sea truth data.

IV. Data anarysis of Orbit #1297, Jan. 26, 1979, off south Japan

IV-1 Preparatory procedure

(1) Range of scenes

The CRT data of the Orbit #1297 contain the following three sequential scenes.

Scene 1. Jan. 26 1979 02h-20m-22s —— 02h-22m-22s (GMT)

Center of scene	25°10′48″N,	137°58′12″E
Corner of scene (NW)	27-05-24 ,	128-53-24
(NE)	29-42-00 ,	145-26-24
(SW)	20-22-12 ,	131-10-12
(SE)	22-49-48 ,	146-50-24

Scene 2. Same bay 02h-22m-22s——02h-24m-22 s (GMT)

Center of scene	32°01′48″N,	136°00′56″E
Corner of scene (NW)	33-04-00 ,	126-17-24
(NE)	36-30-00 ,	144-04-48
(SW)	27-05-24 ,	128-54-00
(SE)	29-42-00 ,	145-27-00

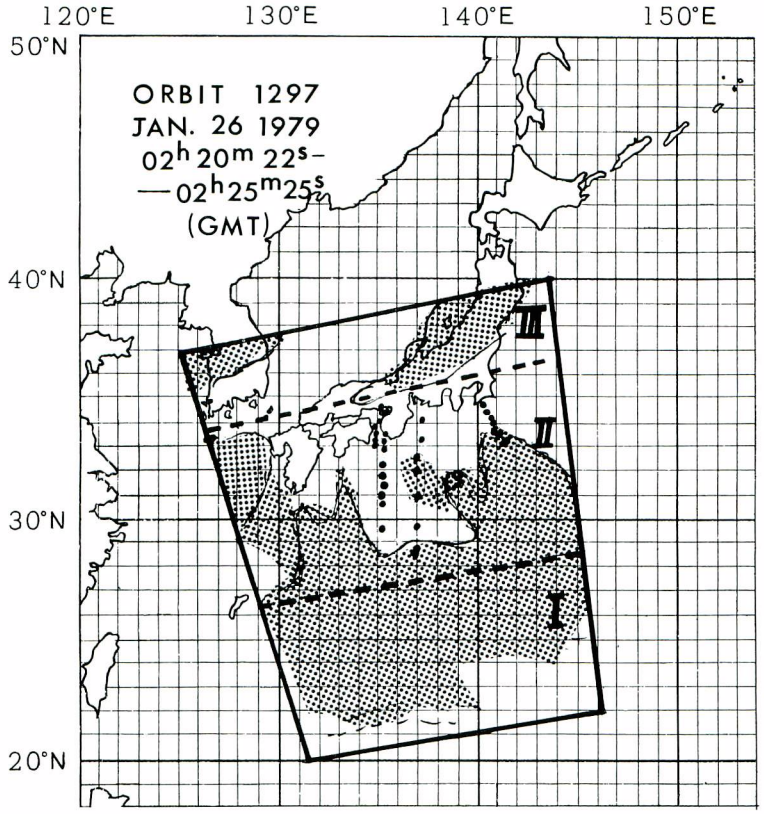

Chart 1. Area covered by the scene of CZCS, Orbit # 1297

Scene 3. Same day 02h-24m-22s —— 02h-25m-25s (GMT)

Center of scene	38°49′12″N,	135°50′24″E
Corner of scene (NW)	40-14-24 ,	125-10-12
(NE)	43-20-24 ,	142-40-12
(SW)	33-42-00 ,	126-17-24
(SE)	36-30-00 ,	144-04-48

Both the Scene 1 and Scene 2 contain 970 scanning lines ; while the Scene 3 does only 512 lines.

(2) Location and posture of the sensor

The altitude of the satellite varies between 947.677 km and 948.236 km in two minutes. The pitch varies between 0.06° and 0.4° with a pseudo period of somewhat around five minutes. The yaw varies slowly between 0.3° and 0.4° ; while the rolling stayed rather still and its amplitude was less than 0.04°. (Fig.3)

(3) Position of the sun

The zenith distance and the azimuth of the Sun at the center of the image is 55.5° and 165.9° respectively.

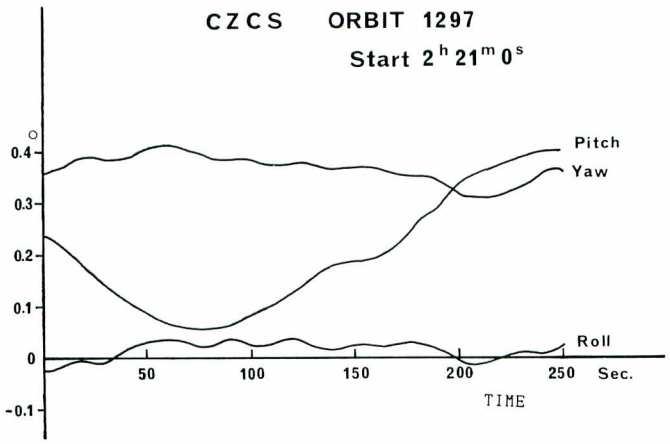

Fig. 3. Location and posture of CZCS, Orbit # 1297

(4) Conversion from radiance count number to radiometric value with the value of the slope a and intercept b in the straight line

$$X = aR + b$$

(X —— radiometric value in mw/sq.cm-ster. μm)

(R —— radiance count number, 0-255)

is tabulated in the following Fig. 4.

Band	a	b
1 (440 nm)	0.03019	0.01670
2 (520 nm)	0.02098	0.03716
3 (550 nm)	0.01713	0.01586
4 (670 nm)	0.00751	0.01253
5 (780 nm)	0.09491	−0.07399

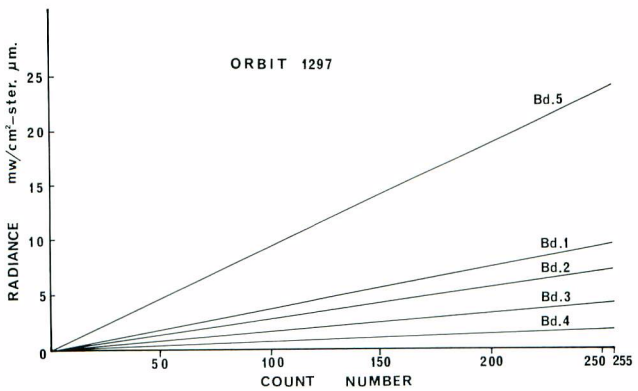

Fig. 4. Conversion from radiance count number to radiometric value of radiance, Orbit # 1297

(5) Conversion of infrared radiance to temperature

The relationship between the radiance count number of the Band 6 and the converted temperature is shown in the Fig. 5.

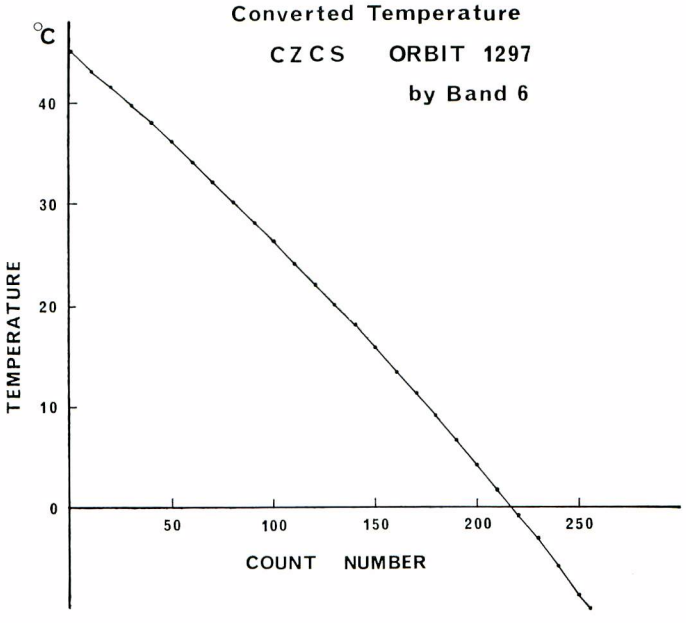

Fig. 5. Conversion from radiance count number of Bd. 6 to temperature

IV-2 Processing of images

(1) Image of each band

The Scene 1 (furthermost south) was found almost overcast. In the Scene 2 and 3 sea surface could be recognized off the Honshu and in the western part of the Sea of Japan off San-in district. The East China Sea in which the sea truth data had been prepared was unfortunately overcast.

(a) Band 1. Most of the land had low radiance (black) ; while the cloud is shown whitish. Two whitish lines run south-eastward from the Cape Ashizuri, the southwest tip of Shikoku Island. Offshore area of the central and eastern parts of Honshu show high radiance and is whitish-gray.

(b) Band 2. The brightness of the land is stronger than that of the Band 1. High brightness is seen in the Seto Inland Sea, Ise Bay and off southeast Honshu. Bright bands run southward in off the Kii and the Bungo Straits respectively. A boundary of brightness can be seen off the San-In district.

(c) Band 3. The pattern is somewhat similar to that of the Band 2. But the land is a little brighter.

(d) Band 4. The land is brighter than in Band 4.

(e) Band 5. The pattern is very different from the above four bands. Brightness of the sea is rather uniform ; while the boundary of the land to the sea is recognizably clear.

(f) Band 6. The sea surface temperature pattern is clearly shown. The shape of the cold ring off Kii Peninsula well coincides to that shown in the oceanographic map prepared concurrently by the Japan Fisheries Information Center (Fig. 6). Moreover, a number of tiny turbulences are indicated along the boundary between the Kuroshio and the coastal water.

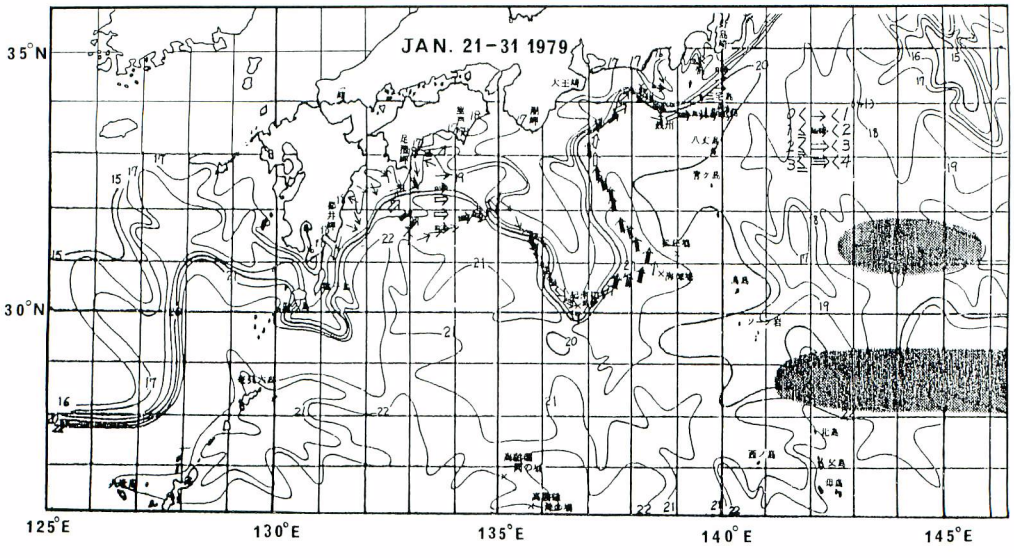

Fig. 6. Surface water temperature map made by vessels data for comparison (after Japan Fisheries Information Center)

(2) Quasi natural colour image (Plate 7).

Blue, green and red are allotted to Bands 1, 2, and 5 respectively, thus making quasi-natural colour display. The yellowish area can be seen in the Seto Inland Sea, the Ise Bay, and at the center of the Sea of Japan, thus indicating the high concentration of chlorophyll in these areas.

(3) Biband ratio image

The false colour display of the ratio R 1/R 2 was made just similar to the case off Baja California done at the preliminary study. In this case a linear transformation

$$R = 300 \times (R\,1/R\,2) - 500$$

was made in order to set the value R between 0 and 255. The histogram of the value R and the biband ratio image are shown in the Fig. 7. and the Plate 12 respectively.

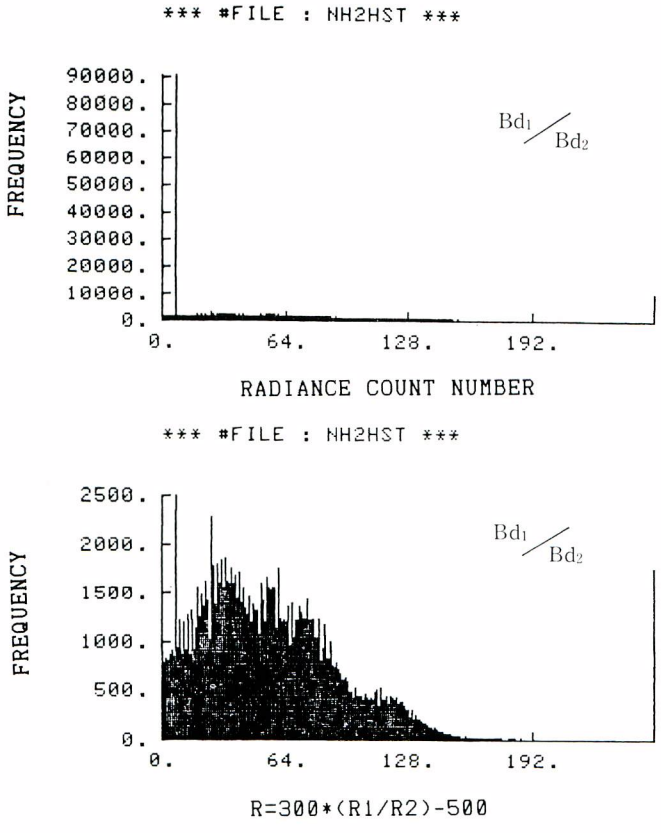

Fig. 7. Histogram of R1/R2, Orbit #1297

The bigger the value of R is, the bigger is the chlorophyll concentration. The reddisher colour was alloted for the bigger value of the concentration. Reddish area can be seen in the Seto Inland Sea and in the Ise Bay just similar to the case of the quasi-true colour picture. A clear front of colour is seen between the coastal water off the Boso Peninsular, south eastern tip of Honshu, and offshore area of it ; thus suggesting a relationship to the distribution of purse seine fishing ground in this area. Another clear front of colour is also seen in the central part of the Sea of Japan. Ohwada (1971) reported that the chlorophyll concentration in the Sea of Japan is bigger in the farther offshore area than in the coastal area. It is however not certain whether the colour pattern of the image can be interpreted as such, because the Ohwada's data, obtained in October 1969 were not synchronized to the satellite data.

It is difficult to tell the land from the sea by the biband image. Therefore, the Band 5 tinted in red was superimposed. As the upward reflectance of this band is very little from the sea, its influence to the ratio is not significant.

IV-3 Comparison to sea truth data

(1) Sea truth data

As has been mentioned, the East China Sea which was originally chosen for comparison was overcast, and accordingly alternate data which had been obtained during January and March 1979 including chlorophyll measurement were selected from the KER Report (Published by the Japan Oceanographic Data Center). They are cruise data of (a) R/V Ryofu Maru, Jan.18-Feb.26, and (b) R/V Shumpu Maru Feb. 26-Mar. 10, both of Japan Meteorological Agency. As the latter ones included a series of repeated observations which were made almost at the same location in the Osaka Bay, they were put together as one ; and thirty stations were taken up as the sea truth data.

As to the index of chlorophyll, the sum of 0 m and 20 m (measured in mg/cub. m) was adopted considering the penetration of the light.

(2) Satellite data

For each station, sampling of satellite data and calculation of relevant statistical data of radiance count of each band was made by means of the software (d) described before. Eight stations among them had count number almost as high as 255. They were considered cloud-coverd and were excluded from analysis. In addition, three stations in the Osaka Bay had extremely high value of chlorophyll concentration. Calculation was accordingly made for two cases namely ; (a) 19 stations excluding those three stations, and (b) 22 stations including them.

(3) Statistical analysis of radiance and chlorophyll

Several types of analyses were tried for obtaining the relationship between chlorophyll concentration and the count number of CZCS, granting that the representability of the statistical value from the latter is not sufficient because the sample size is too small, and also the sea truth stations are not evenly distributed throughout the image.

The air correction was not adopted as the first step of approach. It is to be discussed in the later chapter.

(A) Correlation coefficients between radiance count number and chlorophyll concentration

The logarithm, instead of real number, was adopted for calculation because the anticipated algorithm for estimation of chlorophyll takes the logarithm form. (e. g. Wrigley and Klooster, 1978)

The radiance count R 1 through R 6 show the average on each cluster composed of 25 pixels centered at the sea truth station.

It can be seen that the mutual correlation among R 1 to R 5 are high ; but no significant correlation could be found to the chlorophyll concentration. Meanwhile a pretty high positive value was found between R 6 and Chl-*a*.

The mutual correlation matrix among R 6, Chl-*a*, and sea surface temperature is shown in the Table 2.

Table 1 Correlation coefficients between logrithms of radiance count number and Chl-*a* concentration
(NIMBUS-7 CZCS Orbit #1297, Jan. 26, 1979)

	R 1	R 2	R 3	R 4	R 5	R 6	chl-*a*
R 1	1.000	0.789	0.704	0.791	0.981	0.006	−0.091[a]
R 2	0.788	1.000	0.970	0.943	0.727	0.428	0.236
R 3	0.682	0.961	1.000	0.933	0.665	0.524	0.380
R 4	0.708	0.900	0.916	1.000	0.731	0.243	0.118
R 5	0.744	0.729	0.664	0.702	1.000	−0.054	−0.163
R 6	−0.104	0.249	0.397	0.324	−0.075	1.000	0.781
chl-*a*[b]	−0.220	0.067	0.240	0.254	−0.127	0.885	1.000

Note : (a) The values above the diagonal are concerning the case which excluded the three stations with extremely high value of Chl-*a* in the Osaka Bay.
(b) The values below the diagonal are concerning the case including them.

Table 2. Correlation matrix among R 6, Chl-*a*, and sea surface temperature
(NIMBUS-7 CZCS Orbit #1297)

		R 6	Chl-*a*[a]	SST
	R 6	1.000	0.778	−0.791
(b)	Chl-*a*[b]	0.756	1.000	−0.851
	SST	−0.890	−0.724	1.000

Note : (a) and (b) have the same meaning to the preceding example.

The correlation between the sea surface temperature and chlorophyll can be interpreted without difficulty. The biological productivity off south Japan decreases with distance from the coast while the temperature gets higher.

(B) Empirical formulae estimating chlorophyll concentration (Note : In this report *log* means natural logarithm.

Multiple regression analysis was tried in order to find the relationship between the radiance count numbers from R 1 to R 5 and chlorophyll concentration index C which was defined in IV-3 (1). The Band 6 was excluded from the computation because it is rather different from other bands in its characteristics.

Here r is the correlation coefficient between the calculated and observed values.

(i) $\log C = 9.14 \log R3 - 6.16 \log R4 - 0.58 \log R5 - 13.28$ r = 0.83 case (a)
(ii) $\log C = -6.34 \log R2 + 13.58 \log R3 - 6.16 \log R4 - 5.12$ r = 0.81 case (b)
(iii) $\log C = -6.02 \log R1 + 1.74 \log R2 + 2.33 \log R4 + 25.86$ r = 0.87 case (b)

As to the ratio between radiance count numbers of two bands ;

(iv) $\log C = -7.04 \log (R1/R2) + 1.01$ r = −0.67 case (a)
(v) $\log C = -8.72 \log (R1/R2) + 1.52$ r = −0.46 case (b)
(vi) $\log C = -6.12 \log (R1/R3) + 0.85$ r = −0.79 case (a)
(vii) $\log C = -8.03 \log (R1/R3) + 1.34$ r = −0.58 case (b)

(viii) $log\,C = -8.06\,log\,(R4/R3) + 0.43$ $r = -0.65$ case (a)

As to the combination of two ratios, (in real number, not log.) ;

(ix) $C = -14.08(R1/R3) - 12.81(R4/R3) + 29.98$ $r = 0.86$ case (a)

(x) $C = -63.06(R1/R3) + 83.26(R4/R3) - 11.34$ $r = 0.62$ case (b)

There are many other possible combinations. Only those with significant correlationship were shown here.

Some of the regression lines are shown in Fig. 8. and Fig. 9.

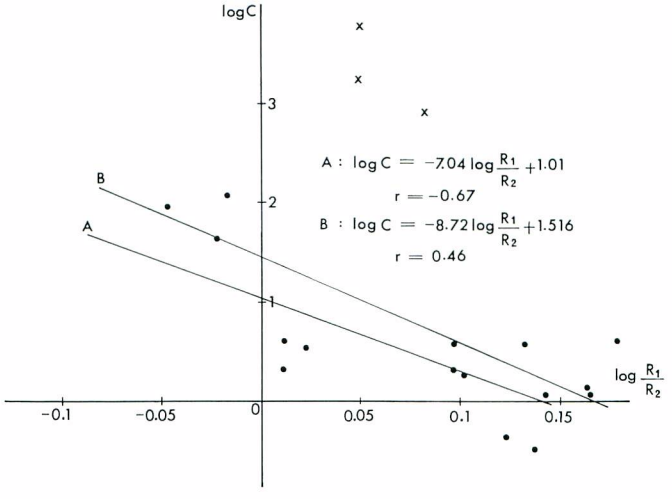

Fig. 8. Regression between chlorophyll concentration and radiance count number ratio of Bands R1 and R2 (both in logarithm)

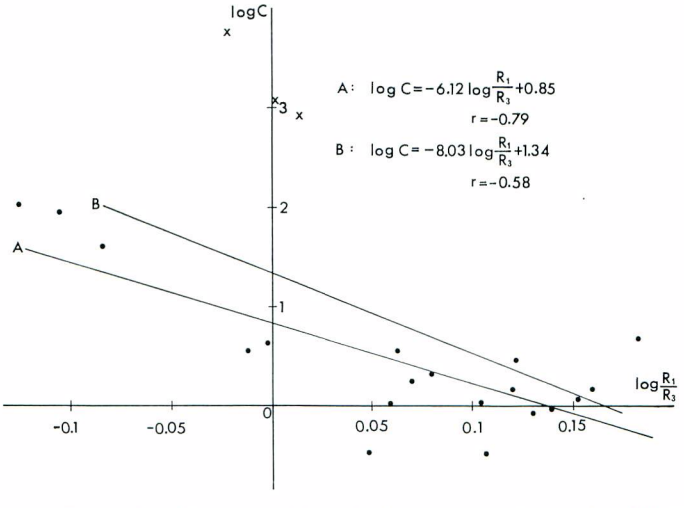

Fig. 9. Regression between chlorophyll concentration and radiance count number ratio of Bands R1 and R3 (both in logarithm)

The lower correlation in the case (b) is due to the extremely high value of the chlorophyll concentration in the Osaka Bay, which is slightly deviated from the reddish part in the picture. On the other hand the high value of chlorophyll seen in the Kii Straits corresponding to the reddish area in the picture contributes the correlationship.

(C) Sum of chlorophyll and phaeopigments

The CZCS cannot identify the chlorophyll-*a* from phaeopigments because both of them have same spectrum character. Therefore the sum of both was replaced to the chlorophyll concentration. Thc correlation coefficient between them in this case is as high as +0.931.

Representing the sum of indices of concentration of chlorophyll and phaeopigments as the "pigment index" and as P, the (vi) and (vii) are transformed as ;

(xi) $log\,P = 1.33 - 3.52 log\,(R1/R3)$ r = 0.80 case (a)

(xii) $log\,P = 1.09 - 5.41 log\,(R1/R3)$ r = 0.62 case (b)

Only slight change was seen in the correlation.

(D) Trial of removing the effect of the cloud

The statistics of radiance count number of pixels centered at the sea truth station show that, (a) The count is all 255 with no standad deviation in the cloud covered area ; (b) The average number is low and the standard deviation is also low in cloud free area. (c) In partly clouded area the standard deviation is high and average is high or low in accordance with whether the area is clouded or clear. (Table 3).

Table 3. Statistical value of radiance count number in clear, overcast, and partly covered areas

	R 1 max.	min.	mean	S. D.	mode	R 3 max.	min.	mean	S. D.	mode
A (Coverd)	255	255	255.0	0.0	255	255	255	255.0	0.0	255
B (Clear)	154	150	152.3	0.8	152	131	125	126.9	1.7	126
C (Mostly covered)	255	167	229.9	34.4	255	255	143	228.4	42.2	255
D (Mostly clear)	255	162	182.1	31.0	168	255	139	168.0	39.1	150

Note : A : St. 8 : 33°33′N, 141°30′E
B : St. 23 : 32-57 , 135-12
C : St. 25 : 31-54 , 135-15
D : St. 3 : 32-41 , 136-59

The minumum value, instead of the average of the radiance count number in each cluster was taken up considering that the minimum would show the sea surface information through the break of the cloud.

By means of this treatment six stations which had been excluded in the former treatment revived in the calculation. The number of available stations in this time is therefore 25 excluding the three stations in the Osaka Bay.

The correlation matrix among the minimum radiance count number of each band and chlorophyll is shown in the Table 4.

Table 4. Correlation matrix among minimum radiance count number in pixel cluster around sea truth station and Chl-*a*

	R 1	R 2	R 3	R 4	R 5	R 6	Chl-*a*
R 1	1.0000	0.8775	0.5314	0.5006	0.6375	0.0069	−0.1253
R 2		1.0000	0.6377	0.4825	0.5794	0.3650	0.1971
R 3			1.0000	0.9318	0.2408	0.5258	0.6190
R 4				1.0000	0.1729	0.2751	0.4421
R 5					1.0000	−0.1216	−0.1691
R 6						1.0000	0.7663
Chl-*a*							1.0000

The correlation coefficient between chlrorphyll concentration and radiance count is highest for R 3 among R 1 through R 5. It is indicated therefore the image of the Band 3 is most suitable for the quick look use.

The correlation coeffcient between chlorophyll concentration and ratio of minimum radiance count number is shown in the following list.

Correlation between chlorophyll concentration and ratio of minimum radiance count number (both in logarithm)

log C	vers	*log* (min. R1/min. R2)	r = −0.64
:		*log* (: R1/ : R3)	: = −0.82
:		*log* (: R1/ : R4)	: = −0.58
:		*log* (: R1/ : R5)	: = +0.16*
:		*log* (: R2/ : R3)	: = −0.52
:		*log* (: R2/ : R4)	: = −0.34*
:		*log* (: R2/ : R5)	: = +0.28*
:		*log* (: R3/ : R4)	: = +0.12*
:		*log* (: R3/ : R5)	: = +0.40
:		*log* (: R4/ : R5)	: = +0.38

Note : Those with * are insignificant at 5 % risk level.

The regression line for the combination with biggest correlation is ;

$$log\ C = -4.45\ log\ (\text{min. R1/min. R3}) + 1.019$$

as is shown in Fig. 10.

(E) Ratio of radiance count number of a band to the sum of all bands (hereafter the minimum radiance count number is used unless special notice)

A trial was made to obtain the correlation between chlorophyll and the ratio RSi = Ri/RS instead of using Ri. Here Ri is the radiance count number of the Band i, RS is the sum of them from Ri through R 5 respectively.

The correlation matrix is shown in the Table 5.

The specific spectrum characteristics of each band and chlorophyll can be observed more clearly here than in the treatment of the radiance count itself. For example the chlorophyll concentration has high negative correlation to R 1 and insignificantly correlates to R 2, while positively correlates to R 3. Thus the black and white pictures of R 1/RS

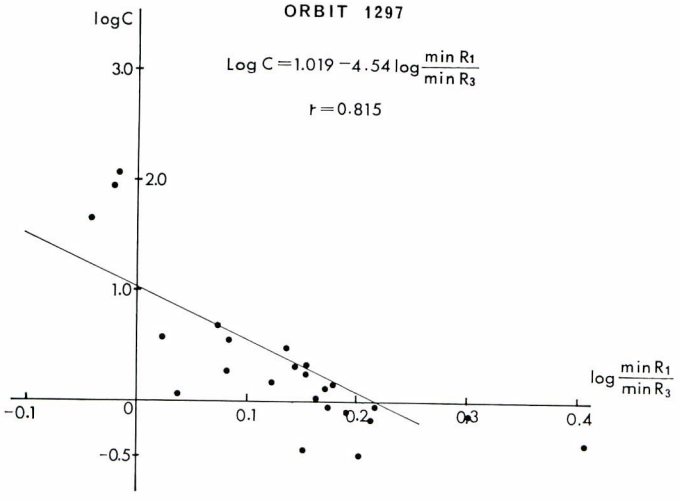

Fig. 10. Regresstion between chlorophyll concentration and minima of count ratio of two Bands R 1 and R 3 (both in logarithm)

Table 5. Correlation matrix between chlorophyll index and ratio of radiance count number of one band to the sum from Band 1 through Band 5, (both data in logarithm)
CZCS Orbit #1297, Jan. 26, 1979

	RS 1	RS 2	RS 3	RS 4	RS 5	C
RS 1	1.0000	0.4646	−0.8761	−0.6009	0.3288	−0.8658
RS 2		1.0000	−0.6557	−0.6598	0.4337	−0.2711
RS 3			1.0000	0.8095	−0.3777	0.7133
RS 4				1.0000	−0.2674	0.3393
RS 5					1.0000	−0.3166
C						1.0000

and R 3/RS would, although they were not actually made, show inverse pattern just as shown in the exercise shown in II-2.

IV-4 Considerations

The data used for calibration as the sea truth adopted here were not completely synchronized to the satellite data ; and they do not cover those waters with high chlorophyll concentration estimated, such as the Seto Inland Sea ; and therefore they are not completely adequate for the comparison.

Besides, it was the mid-winter that the data were obtained ; and therefore the zenith distance of the Sun is big, and accordingly the air scattering might have given large effect.

Thus the results hitherto obtained were rather provisional. However, the fact that the correlationship between chlorophyll and satellite data is as high as 0.8 in absolute value gave us a favorable expectation for the application of CZCS in biological oceanography

and fisheries.

V. Data analysis of Orbit #8774, Jul. 20 1980, the East China Sea

V-1 Preparatory procedure

(1) Provided sea truth data

The oceanographic data of KER obtained by R/V Yōkō Maru were adopted for the sea truth data. (JODC cruise number #49802607)

(2) Range of scenes ; position of the Sun, tilt of the sensor

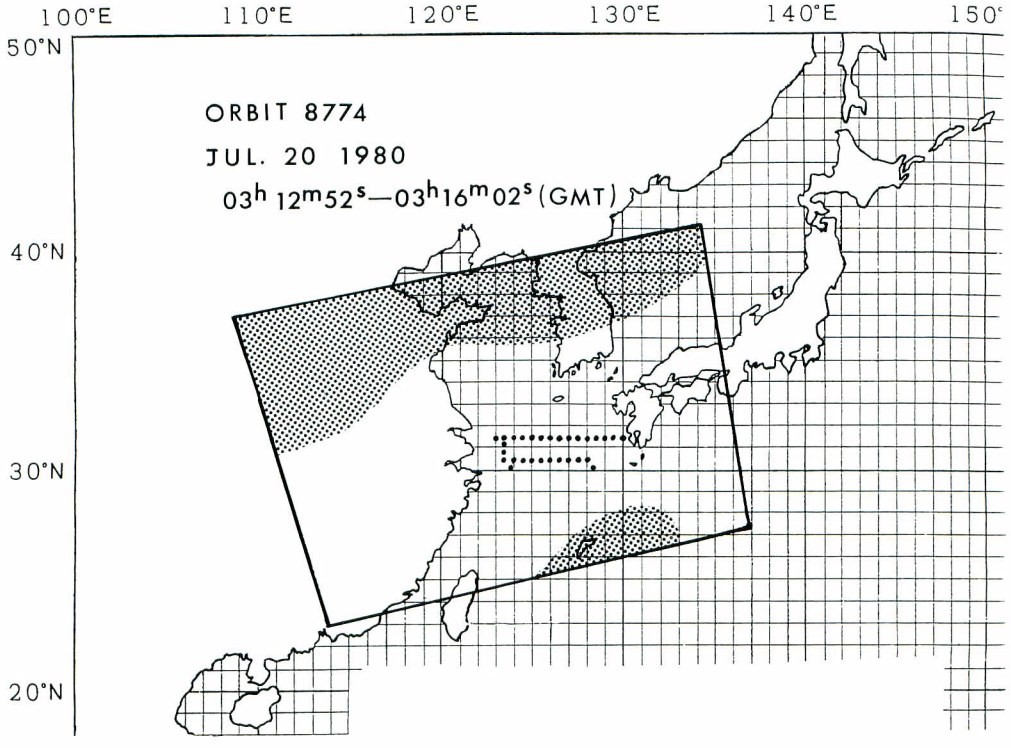

Chart 2. Area covered by the scene of CZCS, Orbit #8774

Scene 1. Jul. 20, 1980, 03h-12m-53s—03h-14m-53s (GMT)

Center of scene	29°11′24″N,	124°18′36″E
Corner of scene (NW)	30-41-24 ,	111-28-48
(NE)	34-36-00 ,	135-55-12
(SW)	24-09-00 ,	114-06-00
(SE)	27-49-12 ,	137-18-00

Zenith distance of the Sun	11.28°
Azimuth of the Sun	175°
Tilt of the sensor	20°

Scene 2. Same day 03h-14m-53s—03h-16m-12s (GMT)

Center of scene	36°0′36″N,	122°14′24″E
Corner of scene (NW)	37-10-48 ,	108-21-36
(NE)	41-22-12 ,	134-55-12
(SW)	30-42-00 ,	135-54-36
(SE)	34-36-36 ,	135-54-36
Zenith distance of the Sun	16.52°	
Azimuth of the Sun	177°	
Tilt of the sensor	20°	

The area of the scene 2 was almost cloud covered.

(3) Location and posture of the sensor

The image location tape was not processed this time because the information of the zenith distance and the azimuth of the Sun, and the tilt of the sensor was already contained in the documentation file.

(4) Conversion from radiance count number to radiometric value

The values of slope a and intercept b in the straight line shown in the chapter IV-1 (1) are shown as follows ;

	Band	a	b
Scene 1	1 (440 nm)	0.04549	−0.00596
	2 (520 nm)	0.03176	0.02117
	3 (550 nm)	0.02666	0.00906
	4 (670 nm)	0.01153	0.02670
	5 (780 nm)	0.09631	−0.14036
Scene 2	1 (440 nm)	0.04538	−0.00170
	2 (520 nm)	0.03166	0.02548
	3 (550 nm)	0.01130	0.01152
	4 (670 nm)	0.01152	0.03837
	5 (780 nm)	0.09600	−0.12496

As the differnce of the parameters amomg the scenes is small, the regression lines of the Scence 2 alone are shown in Fig. 11.

The radiance-temperature relation of the Bd. 6 is shown in Fig. 12. Here again the parameters of the Scene. 1 were employed because there is no substantial difference among the scenes.

V-2 Processing of images

(1) Image of each band

(a) Band 1. — The northern part of the Yellow Sea, and south off Ryukyu Islands are covered by cloud. The coast line of China Continent is in contrast to the black tone of the sea. The gray scale in the sea is hard to identify by this picture alone.

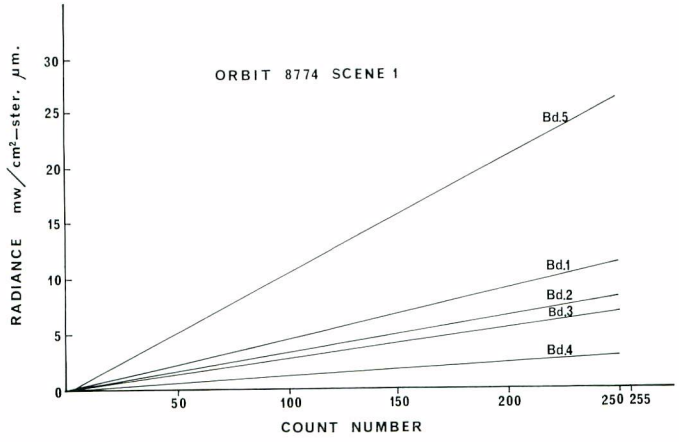

Fig. 11. Conversion from radiance count number to radiometric value of radiance, Orbit #8774

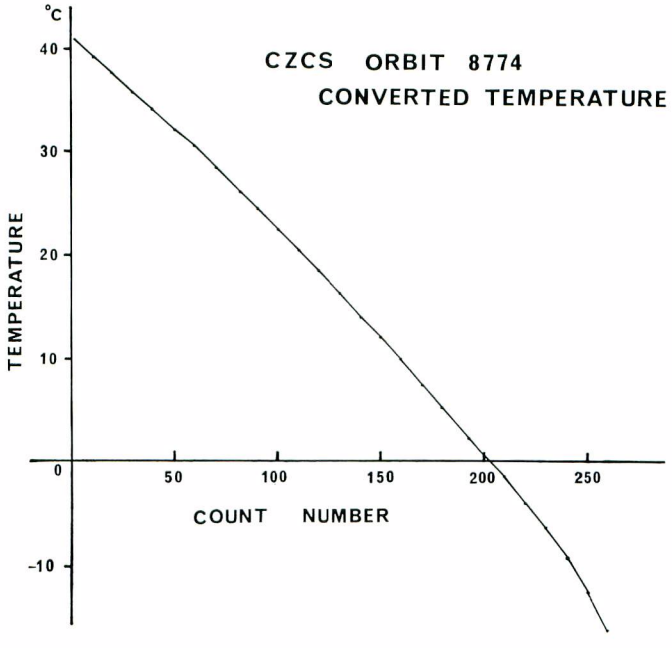

Fig. 12. Conversion from radiance count number of Bd. 6 to temperature, Orbit #8774

(b) Band 2. — The coastal area off Kyushu Island can be recognized more whitish than by the Band 1. Increasing of whitish tone can be seen from the central part of the East China Sea toward the China Continent.

(c) Band 3. — The contrast in tone is a little clearer than the Band 2. Several

fingerlike streaks making clockwise spirals are seen off the estuary of the Chang (Yangzi) River. The Kyushu Island can be seen whitish.

(d) Band 4. — The pattern is rather similar to the Band 3.

(e) Band 5. — Only little information is obtained on the sea except white cloud is seen off South Kyushu. The coastal line is very clear at the western part of Honshu, Shikoku, Kyushu and China ; while the north of the Shangdong Peninsular is covered by cloud.

(f) Band 6. — The surface temperature of the East China Sea is relatively monotonous in summer except the area near Kyushu, where the western boundary of the Tsushima Current is located. Thus the image of this band does not show clear temperature distribution pattern as the case of the North Pacific in winter.

(2) Quasi natural colour image

Blue, green and red were alloted to the Band 1, 3, and 4 in order to generate the quasi-natural colour image.

Most of the western part of Honshu, Shikoku, and Kyushu districts is shown greenish-brown. Blueish tone can be seen off southwestern part of Kyushu and southern part of Shikoku ; while the China continent is show in yellowish brown. (Plate 19)

A geometric correction to the Mercator's projection was also made for the major part of the image. Blueish tone is seen in the south and west of Kyushu. On the other hand it is whitish in the area from the central part of the East China Sea toward the Contient, making a clear colour boundary. The palm-shaped spiral seen at the Band 3 and 4 can also be seen in this picture more clearly. A narrow greenish band is seen along the coast of South China. (Plate 20)

(3) Biband ratio image (Plates 21 and 22)

The ratio, R1/R3, was transformed as

$$R = ((R1+1300)/R3 \times 160 - 460$$

in order to adjust the value of R between 0 and 255 just as the case of the Orbit #1297.

In this time, the parallel and meridian lines are inserted in the image in addition to the geometric correction.

Generally speaking, the reddishness decreases with the increases of the longitude. The purple-blue part surrounding the southern part of Kyushu Isl. corresponds the Kuroshio Water. The area of this colour stretches northward, and breaks at off Nagasaki, and then intermittently extends toward northern Kyushu via Goto Isls. Then it can be recognized again off San-in district, the inside coast of the western Honshu. A clear colour boundary is seen in the middle of the East China Sea. In addition, a set of yellowish fingerlike spiral which extends eastward and turns clockwise from the Hangchow Bay and Jiangsu Province, as well as the reddish area inside of it, is seen in corresponding to the greenish band in the foresaid quasi-narural color picture. Other greenish areas are also seen off northwestern Kyushu and the Bungo Straits. The Band 3 responds not only the reflectance from chlorophyll but also from yellow substance. It is interesting to see

that the yellow-brownish fingers near the coast of the China show the process of diffusion and mixing of the inland water including yellow substance with the open sea water.

V-3 Chlorophyll estimation

(1) Sea truth data

The data source is the JODC Cruise Number #49802607, as was mentioned in V-1 (1).

The concentration of the chlorophyll and phaeopigments is shown in the accumulated value from 0 to 20 m (in mg/cub. m) and hereafter described as "Pigment Index" ,P, as was shown in IV-3, (3), (C).

(2) Satellite data

The minimum value of radiance count number of each band in the cluster of 25 pixels was chosen in the same manner to the former example of the Orbit #1297.

There are 30 sea truth stations ; only one of which was omitted because of cloud cover.

(3) Statistical analysis of radiance and pigments

(A) Correlation coefficient between radiance count number and pigment index (in logarithm)

The correlation matrix among radiance counts of each band and the pigment index is shown in the following Table 6.

Table 6. Correlation matrix among minimum radiance count in pixel cluster around sea truth station and pigment index NIMBUS-7 CZCS Orbit #8774, Jul. 20, 1980

	R 1	R 2	R 3	R 4	R 5	R 6	P
R 1	1.0000	0.7436	0.6184	0.5553	0.4908	0.5691	0.1478
R 2		1.0000	0.9776	0.9508	0.8951	0.7957	0.6790
R 3			1.0000	0.9804	0.9204	0.7884	0.7484
R 4				1.0000	0.9370	0.7463	0.7665
R 5					1.0000	0.7383	0.7717
R 6						1.0000	0.3830
P							1.0000

The inter-band correlation coefficients are generally higher than the case of the Orbit #1297. On the other hand that between the pigment index and Band 6 was rather low in contrast to the former example.

(B) Correlation between biband radiance ratio and pigment index

The following Table 7. shows the result obtained from various combination of bands and pigment index.*

Table 7. Correlation between pigment index and biband radiance ratio of various combinations (NIMBUS 7 CZCB, Orbit # 8774)

log P	vers	*log* (R1/R2)	r = −0.831
:		*log* (R1/R3)	: −0.832
:		*log* (R1/R4)	: −0.816
:		*log* (R1/R5)	: −0.803
:		*log* (R2/R3)	: −0.771
:		*log* (R2/R4)	: −0.781
:		*log* (R2/R5)	: −0.752
:		*log* (R3/R4)	: −0.723
:		*log* (R3/R5)	: −0.675
:		*log* (R4/R5)	: −0.408

(All values are significant at 5% risk level.)

* The value of the correlation coefficient, namely 0.83 in absolute value may not be sufficient for the quantative estimation of the chlorophyll concentration in absolute value, but it is sufficient enough for the estimation of the distribution pattern of it.

The effect of combining two or more ratios in order to use multiple correlation cannot be expected because the correlation among the ratio is high as is shoown in the Table 8.

Table 8. Correlation matrix among biband radiance ratio and pigment index

	R1/R2	R1/R3	R1/R4	R1/R5	R2/R4	R2/R3	R2/R5	R2/R4	R3/R5	R4/R5	Orp
R1/R2	1.0000	0.9838	0.9718	0.9200	0.8868	0.9249	0.8404	0.8719	0.7474	0.3943	-0.8318
R1/R3	0.9838	1.0000	0.9779	0.9135	0.9551	0.9451	0.8382	0.8623	0.7228	0.3660	-0.8321
R1/R4	0.9718	0.9779	1.0000	0.9275	0.9180	0.9884	0.8628	0.9490	0.7649	0.3577	-0.8160
R1/R5	0.9200	0.9135	0.9275	1.0000	0.8373	0.9048	0.9855	0.8704	0.9414	0.6807	-0.8035
R2/R3	0.8868	0.9551	0.9180	0.8373	1.0000	0.9108	0.7748	0.7847	0.6305	0.2929	-0.7730
R2/R4	0.9249	0.9451	0.9884	0.9048	0.9108	1.0000	0.8517	0.9705	0.7534	0.3255	-0.7816
R2/R5	0.8404	0.8382	0.8628	0.9855	0.7748	0.8517	1.0000	0.8272	0.9792	0.7717	-0.7519
R3/R4	0.8719	0.8623	0.9490	0.8704	0.7847	0.9705	0.8272	1.0000	0.7639	0.3150	-0.7229
R3/R5	0.7474	0.7228	0.7649	0.9414	0.6305	0.7534	0.9792	0.7639	1.0000	0.8531	-0.6752
R4/R5	0.3943	0.3660	0.3577	0.6807	0.2929	0.3235	0.7717	0.3150	0.8531	1.0000	-0.4085
(c+p)	-0.8318	-0.8321	-0.8160	-0.8035	-0.7730	-0.7816	-0.7519	-0.7229	-0.6752	-0.4085	1.0000

The multiple correlation of pigment index and all combination of ratio is ;

$$r(m) = 0.841$$

Only a slight improvement in the correlation coefficient was earned. Thus the ratio R1/R3 is sufficient enough for the practical purpose estimating the pigment index.

(C) Empirical formulae estimating pigment concentration

From combinations of bands discussed in the previous section, the highest correlation is obtained in *log* (R1/R3) vers *log* P as ;

$log\,P = 0.5116 - 6.5391\,log\,(R1/R3)$

The regression lines and curves are shown in the Fig. 13 and 14 respectively.

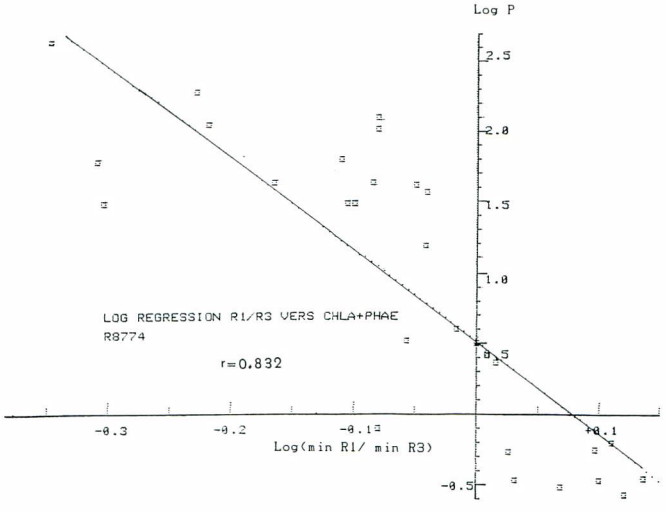

Fig. 13. Regression between pigment index and minima of count ratio R1/R3, (both in logarithm)

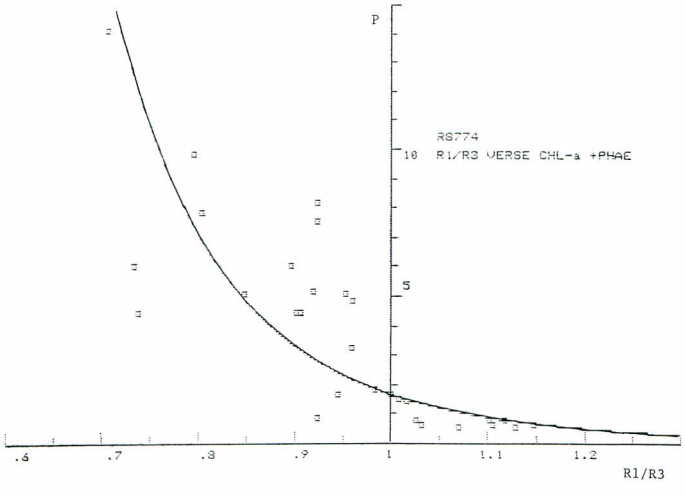

Fig. 14. Regression curve between pigment index and minima of count ratio R1/R3

Adopting the average pigment concentration, P', instead of the accumulated value of the pigment index P, the expression can be modified as,

$$log\ (20P') = 0.5166 - 6.5391 log\ (R1/R3)$$

then $$log\ (P') = 2.479 - 6.5391 log\ (R1/R3)$$

and $$(P') = 0.0838\,(R1/R3)^{6.5391}$$

(D) Ratio of radiance count number of a band to the sum of all bands

Just similar to the case of the data of the Orbit #1297, the correlation between the pigment index and the ratio RSi (=Ri/Rs ; RS=R1+R2+R3+R4+R5) was calculated, the result of which being shown in the following Table 9.

Table 9. Correlation matrix between pigment index and ratio of radiance count number of one band to the sum of it from Band 1 through 5. (both in logarithm)

	RS1	RS2	RS3	RS4	RS5	P
RS1	1.0000	0.9123	−0.7623	−0.9710	−0.8274	−0.8228
RS2		1.0000	−0.6571	−0.9442	−0.7743	−0.7006
RS3			1.0000	0.6552	0.5076	0.7961
RS4				1.0000	0.7982	0.7961
RS5					1.0000	0.7348

In this case the Band 1 and 3 show a reciprocal type of correlation to the pigment index respectively. But the characteristics of the Band 2 as the hinge point is not so clear as in the case of the Orbit. 1297.

If the radiometric value of radiance obtained by using the conversion coefficents shown in V−1 (4) is replaced to the radiance count number, the correlation matrix is modified as the following Table 10.

Table 10. Correlation matrix between pigment index and ratio of radiometric value of one band to the sum of it from Band 1 through 5 (both data in logarithm)

	RS1	RS2	RS3	RS4	RS5	P
RS1	1.0000	0.3279	−0.9260	−0.9636	−0.9012	−0.8237
RS2		1.0000	−0.2479	−0.3750	−0.4649	−0.1563
RS3			1.0000	0.8901	0.7268	0.8079
RS4				1.0000	0.8462	0.7986
RS5					1.0000	0.7726
P						1.0000

In this case the negative correlation of the Band 1 and 3 to the pigment index is also clear. Moreover, the characteristics of the Band 2 as the hinge point is also clear. The correlation between the Band 1 and 3 has a high negative value ; thus clearly showing the reciprocal characteristics of the two bands for the sum of chlorophyll and phaeopigments

(4) Preliminary consideration on the air correction

The radiance measured by optical sensor includes the Reyleigh's and aerosol scattering besides the light from the sea surface.

The procedure proposed by Gordon et al., (1980) is in short ; (a) To adopt the Reyleigh's scattering calculated at the center of the image ; and (b) To obtain the aerosol

scattering at one point in the scene by measuring upwell rabiance from the sea surface and apply it to the whole scene. Namely the procedure is to add an adjustment of a certain value to the measured radiance value.

Accordingly, two parameters A1 and A 3 were chosen and were subtracted from R 1 and R 3 respectively in order to make the correlation coefficient between *log.* (R 1−A 3)/(R 3−A 3) and *log.* P maximum by giving various values. The result is shown in the Fig. 15.

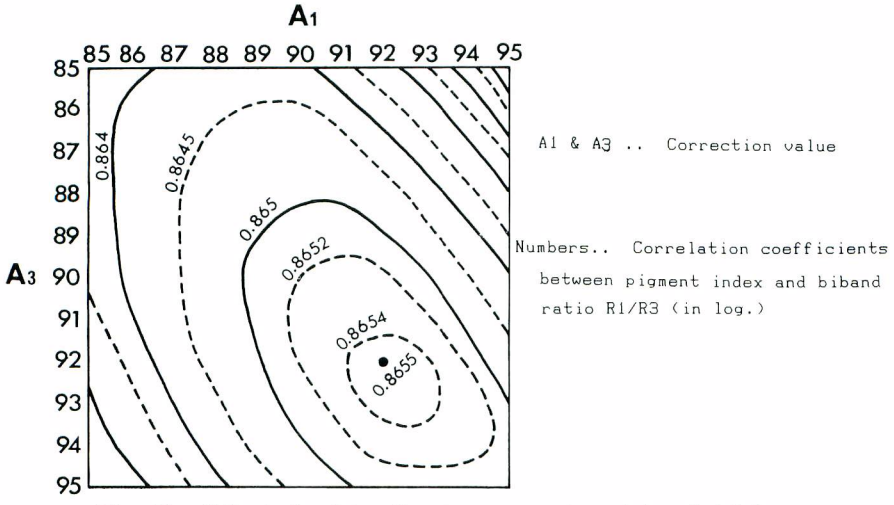

Fig. 15. Effect of subtracting two parameters A 1 and A 3 from radiance count number R1 and R3 respectively for air correction

The maximum value of the correlation coefficient −0.866 was obtained at A1=92, andb A 3 = 92. The effect of such correction was, therefore is not so big.

More detailed discussion on air correction will be made in the latter chapter of this report.

V-4 Comparison with sea truth data

The sea truth data include two parallel lines along 30° 30′N and 31° 30′N respectively. Both lines traverse the Tsushima Current and the boundary of the coastal water along the China Continent. They are thereore adequate to study the profile of oceanographic parameters.

(1) Major currents and water mass distribution in the East China Sea

A schematic description about the water mass and current made by Inoue (1981) is shown in the Fig. 16.

The fundamental oceanographic pattern in the East China Sea can be shown, in short, by three major waters. namely, Kuroshio-Tsushima Current Water which flows from as far south as northwestern off Ryukyu Islands toward north along the continental shelf of China ; the China Continent Coastal Water ; and the Yellow Sea Cold Water. By Inoue's map, the boundary between the first and the second lies along the 100 m bathymetric line and also along the 126°E and 127°E meridans, and then turns southwestward at the northwest off

Okinawa Island at 27°N.

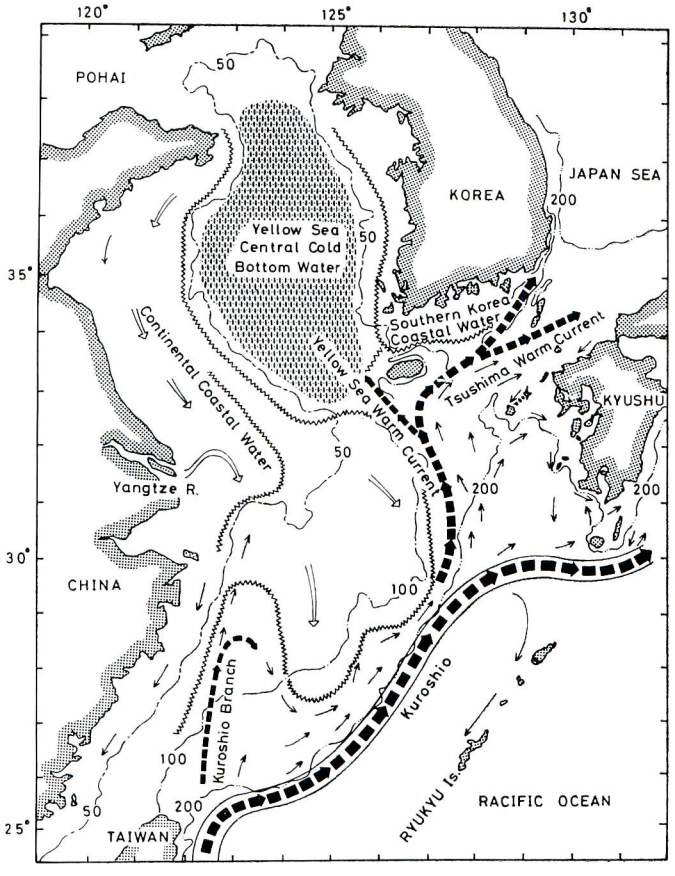

Fig. 16. Schematic expression of hydrography in the East China Sea and the Yellow Sea (after Inoue, 1981)

Another branch of Kuroshio which flows approximately northward on north of Taiwan and, the Continental Coastel Water which flows southward between off Shangdong Peninsular and off the Chang River form another significant oceanographic boundary between 122°E and 123°E, which intrudes eastward off the mouth of the Chang River.

(2) Temperature distribution

The surface temperature in the western part of the East China Sea is in general lower than in the eastern part of it (Fig. 17). But no clear front can be seen in the surface temperature in summer.

The radiance temperature measured by the Band 6 is slightly higher in the neighbourhood of the continent. But no clear pattern of the temperature could be found as was already mentioned in V－2 (1).

The boundary between the Kuroshio and the Yellow Sea Cold Water is, however, clearly seen at 126°E to 127°E at deeper than 30 m in the vertical profile of the sea water temperature (Fig. 18 and Fig. 19).

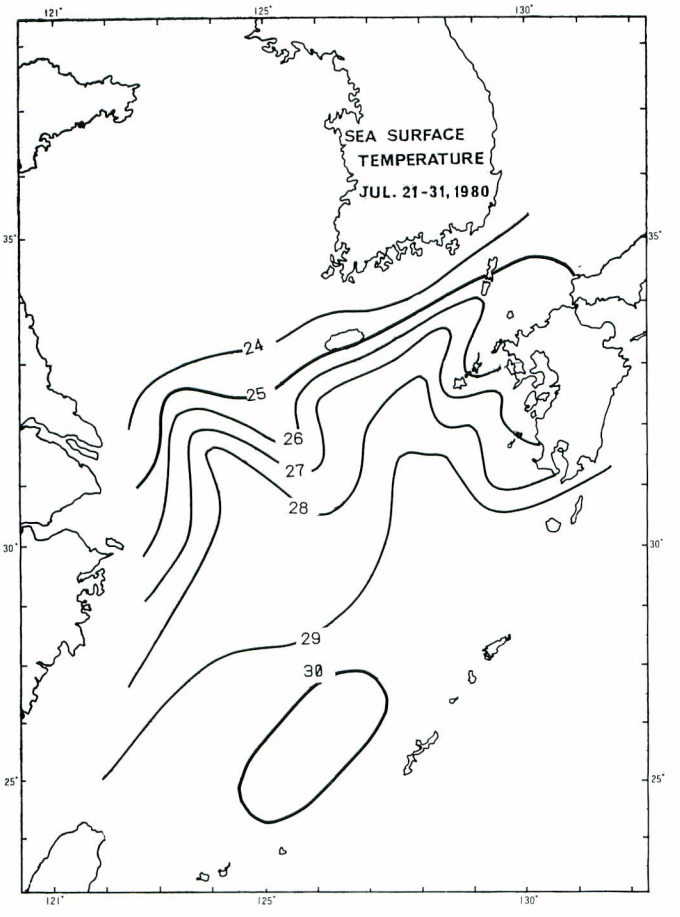

Fig. 17. Sea surface temperature map made by vessels data, July 21-31, 1980

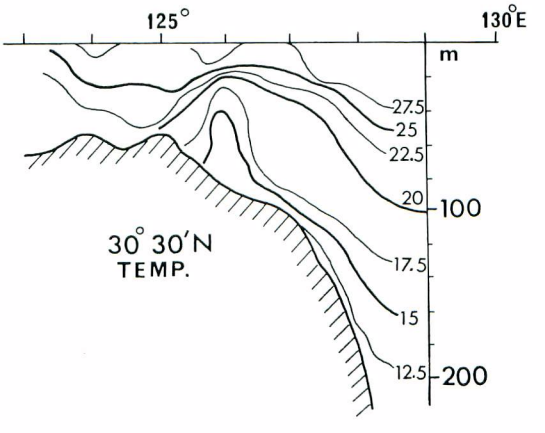

Fig. 18. Vertical profile of temperature along 30°30′N, in the East China, Sea July 1980

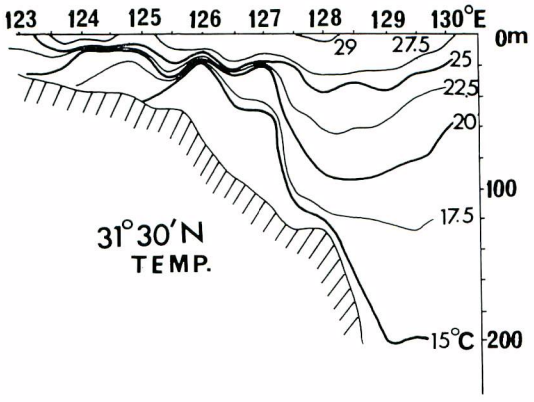

Fig. 19. Vertical profile of temperature along 31°30′N, in the East China Sea, July 1980

The location of the front approximately coincides to that of the colour boundary in the biband picture of R 1/R 3. Moreover the boundary can also be found in the case of monochromatic biband ratio picture of R 1/R 3. (Plate 23).

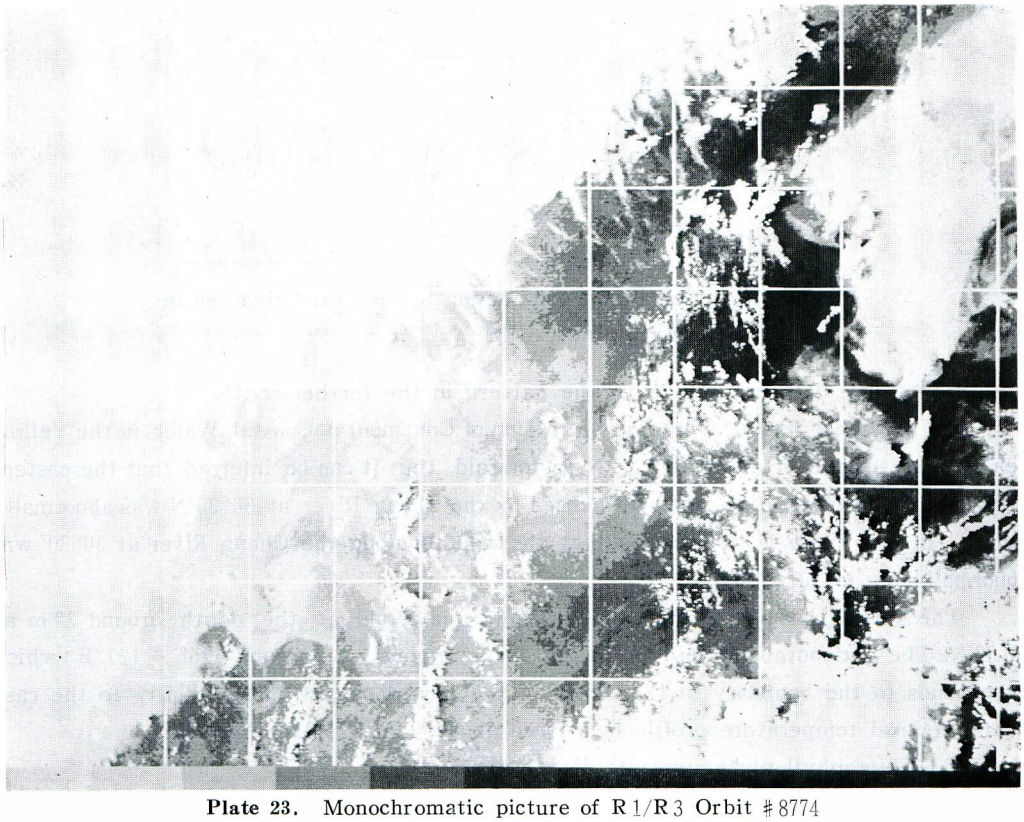

Plate 23. Monochromatic picture of R 1/R 3 Orbit # 8774 (with geometric correction)

It is noteworthy that the CZCS can locate the water mass boundary which cannot be identified by means of the surface temperature distribution pattern.

(3) Salinity distribution

Generally speaking, the eastern part is more haline than in the western part of the East China Sea. In the surface salinity distribution, the gradient along 31°30′N is high at around 125°30′E ; while there is a minimum of surface salinity at around 125°E and its west along 30°30′N. The surface salinity distribution in summer of the East China Sea cited by Inoue (loc. cit.) shows an intrusion of low haline water (<30 ppt.) with its origin at the mouth of the Hunag and Chang Rivers and stretching as far east as 125°E – 126°E at 31°N – 32°N. (Fig. 20).

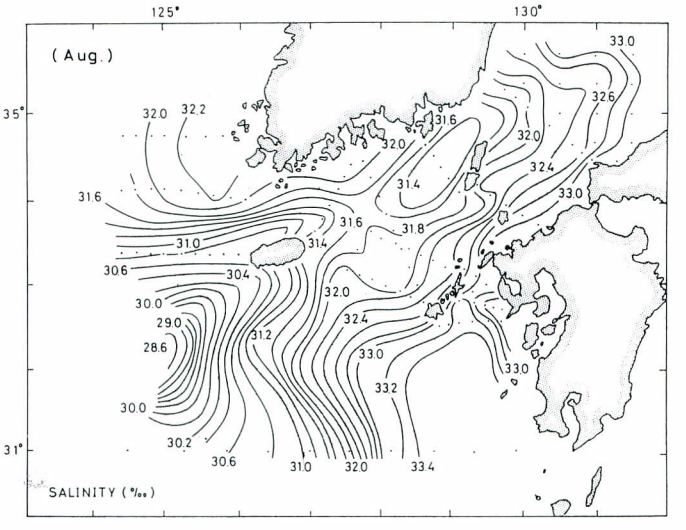

Fig. 20. Surface salinity distribution in the East China Sea in summer, (by Inoue, 1981)

The figure does not deal with the pattern in the farther south.

On the other hand the eastward intrusion of Continental Coastal Water in the Yellow Sea is most significant at around 30°N as foresaid, thus it can be inferred that the eastern intrusion of the low haline water influenced by the Chang River at 30°30′N was abnormally strong, (In fact there is information that the rainfall along the Chang River at 30°30′ was abnormally big in July 1980).

The vertical profile of the salinity show a halocline at the depth around 20 m at 30°30′N. The horizontal gradient in this depth is highest at around 126° – 127°E ; which corresponds to the boundary in the colour of the biband picture just similarly to the case of the vertical temperature profile mentioned above. (Fig. 21 and Fig. 22).

(4) Chiorophyll-phaeopigments distribution

The vertical profile of the sum of chlorophyll-*a* and phaeopigments is shown in the Fig. 23 and Fig. 24.

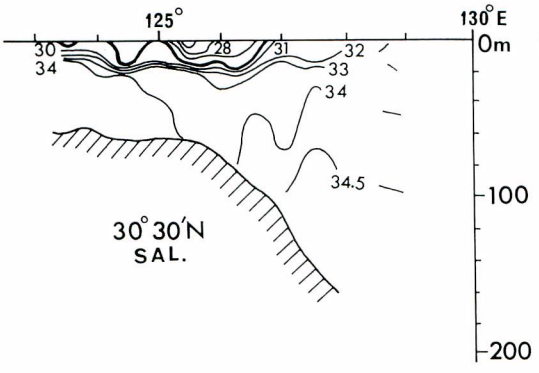

Fig. 21. Vertical profile of salinity along 30°30′N in the East China Sea, July 1980

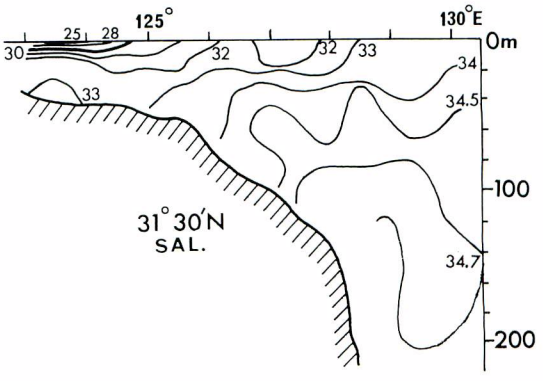

Fig. 22. Vertical profile of salinity along 31°30′N in the East China Sea, July 1680

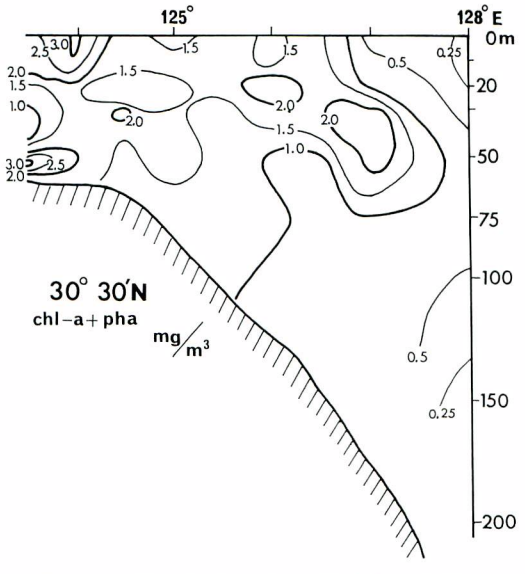

Fig. 23. Vertical profile of chlorophyll + phaeophytin concentration along 30°30′N, in the East China Sea, July 1980

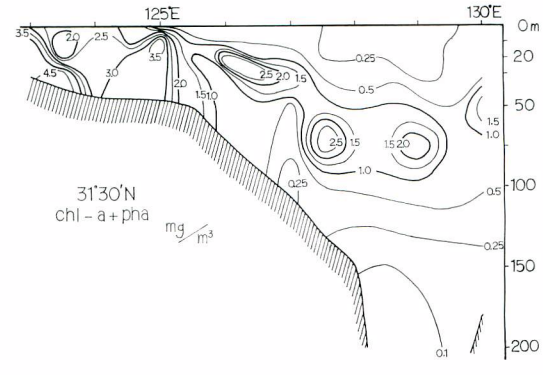

Fig. 24. Vertical profile of chlorophyll + phaeophytin concentration along 31°30′N, in the East China Sea, July 1980

The depth of maximum of the pigment concentration is near the surface in the vicinity of the continent, while it is as deep as 50-70 m in the offshore of Kyushu. The horizontal gradient at the surface is high at 124°E−125°E along 31°30′N, and at 124°E−125°E, and 126°E-127°E along 30°30′N in latitude respectively.

The pigment index (defined in IV-3 (3)) has a similar pattern in the vertical profile A clear boundary of colour from blue to yellowish green can be seen in the P1. 22

at 127°E along 30°30′N line, and at 126°E along 31°30′N line respectively.

Another change of colour tone from yellowish green to blueish green is seen at 125°30′E, and that to reddish purple at 123°E along 31°30′N respectively. In addition, there is a local minimum of the pigment at 124°30′E to 125°30′along the same latitude.

Boundaries of colour tone along 30°30′N parallel can be seen at 126°30′E (from blue to green), and in the vicinity of 124°30′ (from yellow to red) respectively. In addition, there is a local minimum of the pigment index at 124°30′E to 125°30′E along the same latitude.

Those features almost correspond to the change of the value of R1 /R3 as are shown in Fig. 25 and Fig. 26.

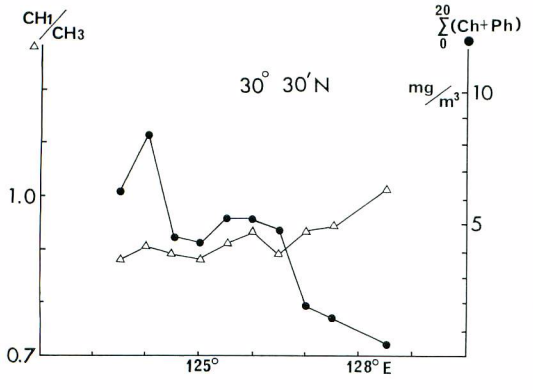

Fig. 25. Comparison of chlorophyll + phaeophytin concentration and the ratio R1/R3 along 30°30′N, in the East China Sea, July 1980

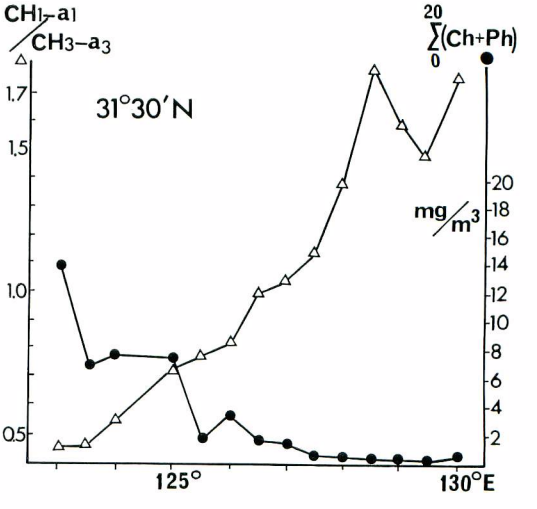

Fig. 26. Comparison of chlorophyll−phaeophytin concentration and the ratio R1/R3 along 31°30′N, in the East China Sea, July 1980

Thus, distribution of the sum of chlorophyll and paeopigments near the surface closely correlates to the value of R1/R3 manifested by colour. And therefore the colour picture may well be said of practical value because it also shows the water mass distribution which cannot be sufficiently depicted by means of temperature alone.

The effluent from continental rivers contains yellow substance and suspended materials besides chlorophyll. They naturally affect the radiance measurement of each band Nevertheless, the rather high correlation of between the pigment index and the radiance ratio leads us a prospect of possibility of estimating the synoptic pattern of the chlorophyll and associated pigment with a good reliability.

(5) Fishing vessel distribution (Fig. 27).

The distribution of purse seine fishing vessels operating in the East China Sea from July 15 through July 24, 1980 is shown in the Fig. 27.

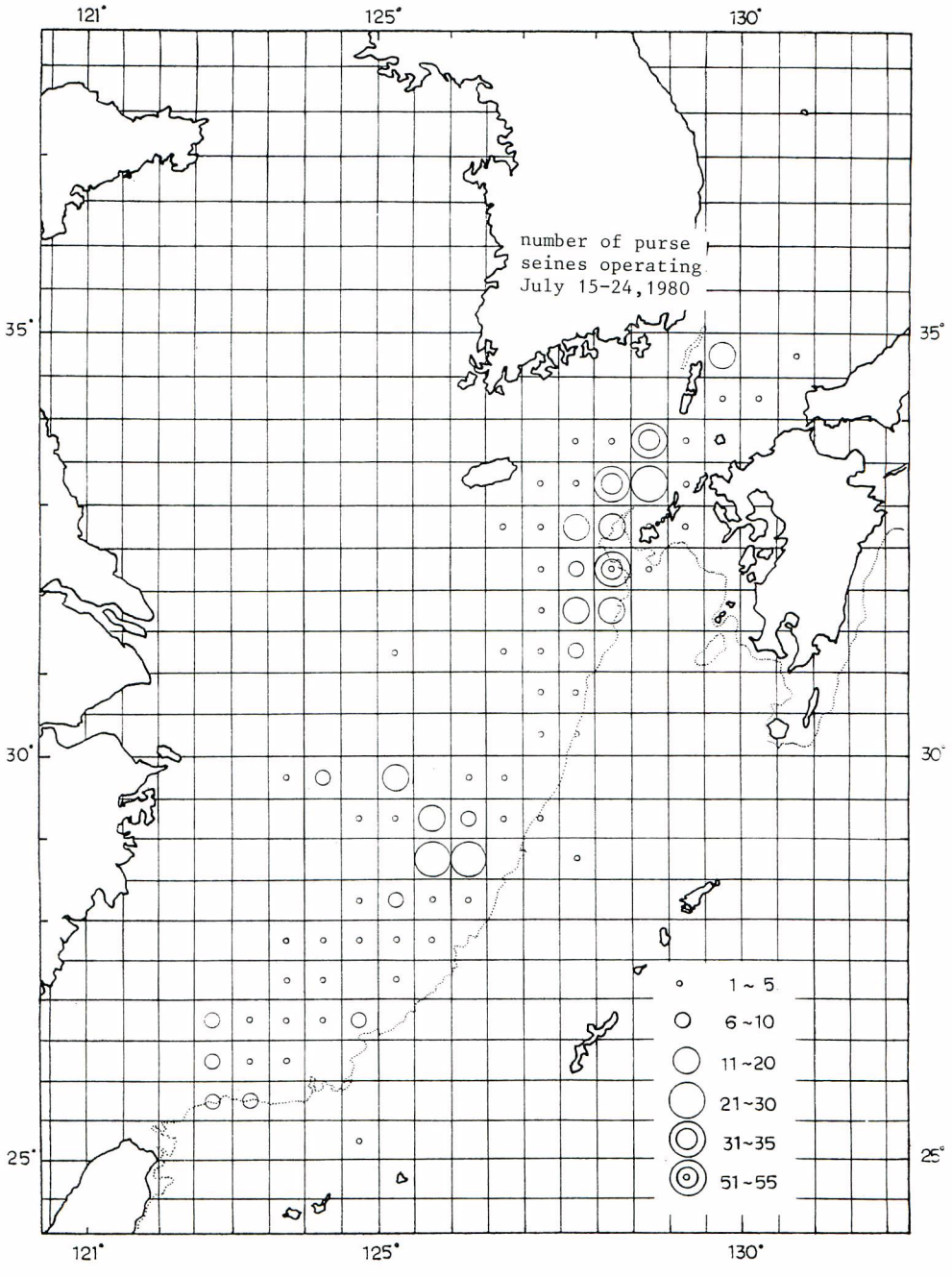

Fig. 27. Purse seine fishng vessel distribution in the East China Sea, July 1980

The distribution of fishing vessels and catch are not always same. But generally speaking, those areas with many boats are good fishing grounds. Comparing the fishing vessels distribution to the colour picture, it is seen that there is a pretty good corresponding between them. The area of dense fishing vessels is seen along the zone of colour boundary ; namely one from dark blue to indigo at off western Kyushu, and one from yellowish green to bluish green at off northwest Okinawa respectively.

VI. Air correction

The radiance measured by CZCS contains, besides the information from the sea, the Reyleigh's scattering caused by gas molecules and the aerosol scattering too.

VI-1. Fundamentel formulae considered

The measured value of the radiance at wave length λ, that is $L(\lambda)$ can be expressed as the following formula, (e. g. Sturm 1980. with slight modification in symbols.

$$L(\lambda) = t(\lambda)\ (Lw(\lambda) + LR(\lambda) + LA(\lambda)$$

here, $Lw\ (\lambda)$, $LR\ (\lambda)$, and $LA\ (\lambda)$ are the radiance due to the sea, Reyleigh's and aerosol scatterings respectively, and $t(\lambda)$ is the transparency ratio from the sea snrface to the sensor.

(1) Reyleigh,s scattering.

In addition to the direct scattering of the Sun beam from the gas molecules of the air, there is also an indirect one caused by the reflection from the sea stuface. The velue of Fresnel's reflection index of the sea water is only about 2% to the incident light vertical to the sea surface and being approximately proportional to the secant of the incident angle. Thus the value of reflection index is 0.029 and 0.04 for 45° and 60° of the incident angle respectively. The indirect scattering was therefore neglected at present analysis against the direct one.

The modified form of the original expression of Sturm for the direct Reyleigh's scattering $Lpr\ (\lambda)$ is ;

$$Lpr\ (\lambda) = (E_o \cdot T_{o3}\ (\mu) \cdot T_{o3}\ (\mu_o) \cdot T_r\ (\lambda)\ /\mu) \cdot PR\ (\psi)$$

The notations used here are :-

$E_o\ (\lambda)$ —— Extraterrestial solar radiance of which values are shown later.

$T_{o3}\ (\mu)$ —— The transparency ratio of ozone and other absorbing materials, namely

$$T_{o3}\ (\mu) = \exp.\ (-\tau_{o3}/\mu)$$

here, $\mu = \cos\theta$; θ is the angle between the view line and the nadir.

τ_{o3} —— The optical depth of ozone.

$\mu_o = \cos\theta_o$; θ_o is the zenith distance of the Sun

T_r —— Reyleigh's optical depth.

$PR\ (\psi) = 3/16\,\pi\ (1+\cos^2\psi)$ —— Phase function of Reyleigh's scattering.

ψ —— Phase angle. And,

$$\cos\psi = \cos\theta\ \cos\theta_o + \sin\theta_o\ \sin\theta_o\ \cos(\phi - \phi_o)$$

ϕ —— The azimuth of the sensor.

ϕ_o —— The azimuth of the Sun.

Various value have been published for the value of Eo, (Table 11).

Table 11. Value of extraterrestrial solar radiance

	Bd 1	Bd 2	Bd 3	Bd 4
Sturm (1981) (1)	185	184	185	153
Austin (1982) (2)	186.42	185.34	184.76	151.52
El Sayed (1982) (3) (cited)	182.5	186.7	196.9	153.6
mean	185.7	185.3	185.6	152.7

Note : (1) —— Attachment 15th NET Meeting Report, Jan. 1981
(2) and (3) — : 18th : : : , Jan. 1982

El Sayed (loc. cit.) considered the seasonal corretion in considering the ellipsity of the corbit of the Earth around the Sun. then

$$E_o(\lambda) = E_o m(\lambda)\ (1 + n\cos^2 A)\ 2 : \qquad n = 0.0167$$

here $E_o m$ = annual mean value of E_o

and $A = 2P\pi d/365$; d is the number of day after the passing of the perihelion (Jan. 2).

The values of the Reyleigh's and gas optical depths adopted by Sturm are as the following Table 12 and Table 13 respectively.

Table 12. Reyleigh's optical depth T_τ (After Sturm, 1981)

Category	1	2	3	4	5
Bd. 1 (440 nm)	0.2329	0.2311	0.2316	0.2300	0.2303
Bd. 2 (520 nm)	0.1231	0.1222	0.1224	0.1214	0.1218
Bd. 3 (550 nm)	0.0969	0.0962	0.0964	0.0956	0.0959
Bd. 4 (670 nm)	0.0444	0.0440	0.0442	0.0438	0.0439

Table 13. Gas optical depth τ_{03} (After Sturm, 1981)

Category	1	2	3	4	5
Bd. 1 (440 nm)	0.0066	0.0067	0.0069	0.0069	0.0071
Bd. 2 (520 nm)	0.0166	0.0200	0.0237	0.0213	0.0275
Bd. 3 (550 nm)	0.0261	0.0323	0.0390	0.0346	0.0461
Bd. 4 (670 nm)	0.0158	0.0191	0.0226	0.0202	0.0264

Note : Category 1 —— Tropic region (0-25°N or S)
2 —— Temperate region (22°-55°N or S), summer
3 —— : : : , winter
4 —— Sub polar region (>55°N or S), summer
5 —— : : : , winter

The value of Reyleigh's scattering at the center of the pictures were calculated with the following results ;

For Orbit # 1297

$\theta = 0°$, $\theta_0 = 45.5°$, $\phi = -9.5°$, $\phi_0 = 165°$

	Bd. 1	Bd. 2	Bd. 3	Bd. 4
E_0	188.33	187.97	188.26	154.88
Lpr (λ)	3.8448	1.9476	1.4806	0.5810

For Orbit # 8774

$\theta = 20°$, $\theta_0 = 17°$, $\phi = -9.5°$, $\phi_0 = 175°$

	Bd. 1	Bd. 2	Bd. 3	Bd. 4
E_0	179.79	179.44	179.71	147.85
Lpr (λ)	4.2627	2.1874	1.6804	0.6508

The radiance count number of each band was converted to the radiometric value.

As is shown in the following Table 14, the Reyleigh's scattering occupies rather major part of the total radiance value.

Table 14. Radiometric value and proportion occupied by Reileigh's scattering

Radiometrie value (mw/sq. cm-ster. μm)		Proportion of Reyleigh's scattering %
Orbit # 1297		
Bd. 1	4.5-6.2	85-62
Bd. 2	2.7-4.2	72-46
Bd. 3	1.8-3.1	82-48
Bd. 4	0.7-1.4	83-41
Orbit # 8774		
Bd. 1	5.7-6.7	85-62
Bd. 2	3.4-5.7	64-30
Bd. 3	2.9-5.4	58-31
Bd. 4	1.0-2.7	65-24

(1) Aerosol scattering

(A) Gordon's algorithm and its application

For aerosol scattering correction we need the *in situ* measurement of the upward radiance at the sea surface of each wave length band. In our present examples, unfortunately however, such data are unavailable. Accordingly a tentative procedure was tried.

In Gordon's method (1981), the "clear water" which contains chlorophyll less than 0.25 mg/cub. m is dealt as the base because it has no upward reflectance of the 670 nm band (Band 4), while that of other hands are determined by the sensor's view angle, zenith distance of the Sun, and Reyleigh's and gas optical depths. It should be noted, however, that the Band 1 has to be dealt in a different way.

Let θ, θ_0, Tr (λ), and τ_{03} (λ) have definition same to the preceding section, the radiance from claer water is, by Gordon ;

$$Lcw\ (520) = 0.495 \cos\theta_o \exp.\ (-\ (T_r/2 + T_{o3})/\cos\theta_o) \quad (1)$$

$$Lcw\ (550) = 0.280 \cos\theta_o \exp.\ (-\ (T_r/2) + T_{o3})/\theta_o) \quad (2)$$

$$Lcw\ (670) = 0 \quad (3)$$

The upward radiance over the clear water is ;

$$t(\lambda)\ Lw\ (\lambda) = Lcw \exp.\ (-(0.5\ T_r + \tau_{o3})\ \sec\theta) \quad (4)$$

λ = 520 nm, 550nm, 670 nm

Therefore the aerosol scattering $L_A\ (\lambda)$ can be expressed as ;

$$L_A\ (\lambda) = L\ (\lambda) - L_R\ (\lambda) - t\ (\lambda)\ L_W\ (\lambda) \quad (5)$$

$$\text{Putting } S(\lambda, \lambda_o) = L_A\ (\lambda)/L_A\ (\lambda_o) \quad (6)$$

for λ_o = 670 nm

and also ;

$$S\ (\lambda, \lambda_o) = (E_o\ (\lambda) \exp.\ (-\tau_{o3}\ (\lambda)\ (\sec\theta + \sec\theta_o))/ (E_o\ (\lambda_o) \exp.\ (\tau_{o3}\ (\lambda_o)\ (\sec\theta + \sec\theta_o))e\ (\lambda, \lambda_o) \quad (7)$$

or ;

$$e(\lambda, \lambda_o) = S\ (\lambda, \lambda_o)\ ((E_o\ (\lambda) \exp.(-\tau_{o3}\ (\lambda)\ (\sec\theta + \sec\theta_o))/ (E_o\ (\lambda) \exp.(-\tau_{o3}\ (\lambda_o)\ (\sec\theta + \sec\theta_o)) \quad (8)$$

$$\text{Putting } e\ (\lambda, \lambda_o) = (\lambda_o/\lambda)^{n(\kappa)} \quad (9)$$

or ;

$$n\ (\lambda) = \log\ (e\ (\lambda, \lambda_o))/\log\ (\lambda/\lambda_o) \quad (10)$$

The value of $n\ (\lambda)$ can be obtained for λ = 520 (Band 2) and λ = 550 (Band 3). For the Band 1 (440 nm), Gordon's method applies ;

$$n\ (448) = (n\ (520) + n\ (550))/2 \quad (11)$$

then

$$e\ (440, 670) = (440/670)^{n\ (440)} \quad (12)$$

can be calculated : and furthermore ;

$$S\ (440, 678) = (E_o\ (440) \exp\ (-\tau_{o3}\ (440) \sec\theta + \sec\theta_o))/ (E_o\ (670) \exp\ (-\tau_{o3}\ (670) \sec\theta + \sec\theta)) e\ (440, 670) \quad (13)$$

and the aerosol scattering of the Band 1 can be obtained by ;

$$L_A\ (440) = S\ (440, 670)\ L_A\ (670) \quad (14)$$

(B) Example of Gordon's method application to CZCS data

(a) Orbit # 1297 (Off South Honshu, winter, 1979)

Time and date	02—20/25Z 26—01—79	
Zenith distance of the Sun	θ_o	44.9°
Azimuth of the Sun	ϕ_0	167
Zenith distance of the view axis	θ	0
Azimuth of the view axis	ϕ	−9.5

by above ;

View angle	τ	44.9
Phase function	P_R	0.0896285

As to the clear water the St. 4 and 5 at which the chlorophyll concentration were

the least among the survey data, although the value was about 0.3 mg/cub. m, a little excceding the criterion.

From (1) to (3) ;

Clear water radiance Lcw(λ) is ;

Lcw(λ) ; Bd. 2 —0.31102, Bd. 3 — 0.17536, Bd. 4 — 0.0000

From (5) the aerosol radiance over the clear water LA (λ) is ;

LA (λ) : Bd. 2 — 0.68892, Bd. 3 — 0.71020, Bd. 4 — 0.38955

By (6) S (λ, λ_0), = 670 nm is ;

S (520, 670) = 1.76849 ; S (550, 670) = 1.82311

By (8) ;

e (520, 670) = 1.46104 ; e (550, 670) = 1.56037

By (10) ;

n (520) = 1.49495 ; n (550) = 1.55037

For Band 1 ;

n (440) = (n (520) + n (550))/2 = 1.87517

Then ;

e (440, 670) = 2.20012 and

S (440, 670) = 2.77053

LA (440) = 1.08239

In this case the value of radiance over the clear water is ;

t (λ) Lw (λ) = L (λ) − Pr (λ) − La(λ) = 4.9085 − 3.844 − 1.082 = −0.0175

that is, the value of the radiance from the sea surface was estimated as negative.

(b) Orbit # 8774 (East China Sea, July, 1980)

Time and date	03—12/15Z,	17—20—80
Zenith distance of the Sun	θ_0	17°
Azimuth of the Sun	ϕ_0	175
Zenith distance of the view axis	θ	20
Azimuth of the view axis	ϕ	−9.4
View angle	ψ	36.97
Phase function	Pr (ψ)	0.0977784

Clear water radiance Lcw (λ)

Lcw (520) = 0.43488, Lcw (550) = 0.24617, Lcw (670) = 0.0000

Radiance over clear water t(λ) Lw (λ) ;

Bb. 2 ··· 0.39952, Bb. 3 ··· 0.22632, Bb 4. ··· 0.0000

In this case seven stations, namely St. 1—St. 7 were used as the clear water stations, at which the average value of chlorophyll-*a* from 0 m to 20 m was below 0.25 mg/cub. m. Then ;

Measured radiance over clear water L (λ) ;

L (520) = 6.01552, L(550) = 3.62152, L(670) = 1.5090

Aerosol radiance over clear water La(λ) ;

$L_A(520) = 1.03464$, $L_A(550) = 1.09329$, $L_A(670) = 0.49482$

Value of $S(\lambda, \lambda_0)$;

$S(520, 670) = 2.09095$, $S(550, 670) = 2.2095$

Value of $e(\lambda, \lambda_0)$;

$e(520, 678) = 1.72612$, $e(550, 670) = 1.86913$

Value of $n(\lambda)$;

$n(520) = 2.15379$, $n(550) = 3.16920$

For Band 1 ;

$n(440) = (n(520) + n(550))/2 = 2.661149$

$e(440, 670) = 3.0623$

$S(440, 670) = 3.82256$

$L_A(440) = 1.89146$

Therefore,the value of radiance over clear water is ;

$t(\lambda) Lw(\lambda) = L(\lambda) - P_R(\lambda) - L_A(\lambda) = 6.0155 - 4.26269 - 1.89146 = -0.13865$

The value is negative again.

Thus the value of path radiance obtained by applying Gordon,s method exceeds, in both examples, the measured value of radiance, thus gave rather absurd result. The reason may be considered, firstly, there is no *in situ* measurement of $t(\lambda) Lw(\lambda)$, and therefore various parameters applied in this calculation may not be applicable for the area different from that where they were obtained ; and secondly the stations which were taken as clear water might not be adequate for the purpose,

VI-2 Comparison of the obtained parameters to other results

Sturm (1982) obtained the value of $e(\lambda, 670)$ in Adriatic Sea both by calculation and observation, the result being shown in the following Table 15.

Table 15. Value of $e(\lambda, 670)$ in Adriatic Sea (Sturm 1982)

Date	Wave Length (nm)	$e(\lambda, 670)$ (Cal.)	Number of Pixels	S.D.	$e(\lambda, 670)$ (obsd.)
Jul. 7, '79	443	1.958	6	0.102	2.19+−0.22
	520	1.547	6	0.047	1.62+−0.16
	550	1.351	6	0.037	1.45+−0.15
	670	1.000	—	—	1.00
May 6, '79	443	2.371	9	0.194	1.97+−0.3
	520	1.741	9	0.068	1.53+−0.15
	550	1.479	9	0.078	1.39+−0.14
	670	1.000	9	—	1.0

In addition, the same author also published the following values in the same area in different period.

Apr. 2 1979 $e(440, 670) = 2.442$

$e(520, 670) = 1.759$

e (550, 670) = 1.525

Apr. 3 1979 e (440, 670) = 2.824

e (520, 670) = 1.886

e (550, 670) = 1.643

The data were obtained by satellite alone without air data.

The following Table 16 is the compiled list of the value of e (λ, 670), obtained by several authors including the present report.

Table 16. Comparison of values of e (λ, 670) by various authors

λ	Gordon Gulf Nov. '81	Sturm (1) Ador. Sea Jul. '79	Sturm (2) Ador. Sea May '79	Sturm (3) Ador. Sea Apr. '79	Sturm (4) Ador. Sea Apr. '79	Yamanaka et al (1) North Pacific Jan. '79	Yamanaka et al (2) East China Sea Jul. '88
448	1.38-1.41	1.958	2.371	2.442	2.824	2.228	3.862
518	1.14-1.46	1.547	1.741	1.759	1.886	1.461	1.726
558	1.06-1.25	1.351	1.479	1.525	1.643	1.560	1.869

The values obtained by Gordon are the lowest, and those of the present report is the highest particularly in the summer of the East China Sea.

VI-3 Consideration of air correction from practical viewpoint

As was mentioned above, it was not completely successful to obtain the good result of air correction by present examples. One of the possible reasons may be that the foresaid Gordon's algorithm and relevant optical parameters might not be valid for Japanese waters. From the viewpoint of practical application for fisheries, it is useful enough if we can know the distribution of chlorophyll or water mass by means of more simple procedure.

Uno (1978, 1979, 1980) measured chlorophyll in the Seto Inland Sea by a MSS equipped on an aircraft. The correlation coefficient hetween the logarithm of chlorophyll concentration C and the logarithm of the ratio Ri/RS was obtained. Here Ri is the radiance count of the i-th band and SR is the sum throughout eight channels from 380 nm to 1100 nm.

The correlation coefficient between log C and log (R3/RS), (450—500 nm) was as high as 0.9 and that between *log C* and *log* (R7/RS), (660—690 nm) was 0.8 in absolute value respectively, eventhough no special procedure was applied for air correction. This method, namely, summing up radiance count number of various wave length bands, can be interpreted to consider the denominator as the white colour and smoothing noise effect of each band.

The aircraft survey, made in rather low altitude, may well be considered somewhat different the case of CZCS. But as has been already mentioned, the correlation between the *log* C or *logs* P and *log* (Rl/RS) or *log* (R3/RS) was higher than those obtained by using R 1 or R 3 themselves, for both cases of the Orbit # 1297 and # 8774.

The alternate results, obtained by using the converted radiometric value instead of the radiance count number is shown in the Table 17 (For the Orbit # 8774 it has been already shown as Table 9.)

For both cases the correlation between the pigment concentration and the ratio R3/RS is high. The characteristics of the Band 2 as the hinge point is clearly shown, except the case of radiance count of the Orbit # 8774.

On the other hand the correlation coefficient using the ratio R1/RS shown in radiometric velue is inferior to that of the count number in the Orbit # 1297. Such difference is considered being due to the difference of the optical charactreristics by season because of the seasonal change of atmospheric conditions. Further studies are required by accumulating more data both for season and area.

Table 17. Correlation matrix between chlorophyll index and ratio of radiometric value of radiance of each CZCS Band i to the sum of them from Band 1 through 5.

CZCS Orbit # 1297						
	R 1	R 2	R 3	R 4	R 5	C
R 1	1.0000	0.2331	−0.2354	−0.2555	−0.4705	−0.5681
R 2		1.0000	−0.1386	−0.3776	−0.2717	0.1091
R 3			1.0000	0.8551	−0.6676	0.7093
R 4				1.0000	−0.4964	0.4529
R 5					1.0000	−0.2632
C						1.0000
CZCS Orbit # 8774 (same table as Table 10)						
	R 1	R 2	R 3	R 4	R 5	P
R 1	1.0000	0.3279	−0.9260	−0.9636	−0.9012	−0.8237
R 2		1.0000	−0.2479	−0.3750	−0.4649	−0.1563
R 3			1.0000	0.8901	0.7268	0.8079
R 4				1.0000	0.8462	0.7986
R 5					1.0000	0.7761
P						1.0000

Note : In the Orbit # 8774, pigment index P was used instead of chlorophyll index C. (IV-3(1).)

In Gordon's method the scattering is dealt uniform throughout the image. In fact, however, there might be much heterogenuity in it. And moreover there may be rather high correlation among the path radiance among each wave length band. In such case, the ratio of the radiance between different bands will make help to compensate the disturbance of path radiance to some extend ; and thus such picture made by using the ratio Rl/RS is more adequate to show the distribution pattern of the chlorophyll than that using only one wave lenghth band directly, even for the purpose to study the picture of the pattern of radiance distribution of a cartain band, say, for example the Band 1.

The case of the ratio between two bands such as R 1/R 3 is basically quite similar to Ri/RS for compensation of the path radiance effect.

Accordingly, the ratio picture of R3/RS (preferably using the converted radiometric-value), or that of R1/R3 are considered adequate means to represent the chlorophyll distribution pattern from the practical viewpoint of fisheries because of the readiness of the procedure

eventhough there is not sufficient corresponding data concerning the air path radiance.

VII. Problems for future study

VII-1 Collection of air correction data

The *in situ* measurement of upward radiance of various wave length needs to be made at the same area to the CZCS data at the similar sun elevation even if both sets of data are not synchronized.

VII-2 Processing more data

Up to date only two scenes have been analyzed because we had to select out only most adequate data by the criteria mentioned in III, and therefore we could not trace the seasonal variation of the chlorophyll concentration of the same area. As the matter of fact, however, although there are a bulk of oceanographic data around Japan, only few of them include chlorophyll measurement, much less, in synoptic wide area which adequate for sea truth data for the study of CZCS data.

On the other hand, the CZCS data are worth while to be procesed if they contain some clear area with remarkable colour boundaries, or it they contain some area adjacent to that already processed, eventhough there are no suitable sea truth data for calibration. It is therefore urged to process more data as far as they are available.

VII-3 Quick processing of data

There are two aspects of the application of CZCS data for fisheries. The synoptic study of marine biological productivity ; and to give us oceanographic information besides water temperature which has directly much to do with fisheries, such as water mass distribution and boundaries between them.

The former of is more or less academic and does not always require real time data processing ; whereas the latter has no practical value without a real time processing and dissemination of data.

In the former the quantitative accuracy is required, and careful calibration with sea truth data should be done as far as possible. For the latter, however, it is unpractical to expect such troublesome treatment of sea truth calibration and air correction every time. It is practically sufficient enough to use the biband ratio picture.

VII-4 Successor of CZCS

NIMBUS-7 has been already on orbit five years. The sensor is now being weakened gradually. we cannot therefore expect much more data before a similar satellite will be on orbit some near future.

Japanese Marine Observation Satellite MOS-1 which will be launched in 1986 is equipped with MESSR. Its wave length band and view range are both similar to LANDSAT series and therefore its application to the fisheries is expected only in limitted field. For

fisheries we need the sensor with narrow spectrum band, wider view area, and more frequent returning just as CZCS for detecting chlorophyll powerfully in synoptic field.

It should be also encouraged to develop research using the similar sensor using an aircraft or in the laboratory for basic simulation studies.

Remarks and acknomledgement

The research was carried out within the framework of the Japan-U. S. A. Cooperative Programme in Science and Technology in Non-Energitic Field, and was financed by the special arrangement of the Japan Science and Technology Agency.

Among the authors Yamanaka took part as the Contact Point Officer of the project with NASA, and was engaged in statistical analysis of CZCS and sea truth data. Hosomura took part in developing of software for the CZCS data processing and photographing of the processed data. and Kozasa did in preparing sea truth date and in discussion on the oceanographic conditions of the East China Sea.

The authors express their heartily thank to Prof. T. Sakata, the Director of TRIC, and his associates for providing every convenience in using their facility ; and also to Prof. Y. Sugimori for his continual valuable advices in conducting the research. The authors also express high gratitude to the cooperation of Dr. S. Wilson and his colleagues in NASA in providing CZCS data and many useful ralevant information.

Acknowledgement should be also made for Dr. H. Ōtaki, Far Seas Fisheries Research Laboratory, who endeavored to edit the manuscript after the retirement of Yamanaka from the governmental service.

Summary

This report deals with the results obtained by 1982 on the Marine Resources Study by means of NIMBUS CZCS which was started in 1979 as one of the Cooperative Projects initiated under Japan - U. S. A. Cooperation in Science and Technology in Non-Energy Field.

As the arrival of data tape was much delayed than the original schedule, the data tape of the waters off western coast of America was purchased tentatively and development of relevant software for image processing were made (Pl. 1-4). The biband picture of the Band 1 and 3 was suggested to be associated to the chlorophyll distribution.

Among the fifteen sets of data tape arrived by 1981, two sets were selected out for further analysis by selection based on cloud covering of the image.

(1) Orbit #1297 (South of Honshu, Jan. 26, 1979).

Pictures of each monoband, synthesized false colour, and biband of the Band 1 and 2 were made by applying the software developed in the preceeding year (P l. 6—12). Additional software was made so as to sample out the pixels around sea truth points and calculate the statistics of the radiance count pertaining to the pixel clusters. Data of observation by the vessels of Japan Meteorological Agency were adopted as the sea truth

data.

The infrared picture (Band 6) clearly shows the meandering of the Kuroshio off the Kii Peninsula, which is well conformed to the result obtained from vessels data (P 1. 10, Fig. 6)

Various statistical analyses were tried on the correlationship between the sea truth and satellite data. After removing the effect of cloud to some extent by means of the pattern of radiance count in the pixel clusters centered ot the sea truth points, the relation

$log\ C = 4.54\ log\ (\text{min. R1}/\text{min. R3}) + 1.019$

(Hereafter "min." is omitted unless special need takes palce.)

stands for the average concentration of chlorophyll-*a* between 0 and 10 m., and the radiance count number R 1 and R 3 for the Band 1 and 3 respectively. The correlation coefficient between *log* C and *log* (R1/R3) was −0.82 (Fig. 10). The correlation between *log* C and *log* (R1/RS) (RS is the sum of radiance count number through Band 1 to 5) is high for the Band 1 and 3 with reciprocal sign ; while low for the Band 2 which is so-called the "hinge point" (Tab. 5).

(2) Orbit #8774 (West of Kyushu, July 20, 1980).

Pictures were processed just similarly to the former case. (P1. 13−19. P1. 21).

Additional software to insert meridian and parallel lines to the picture and to transfigure the image into the Mercator's projection were developed. (P1.20, 22, 23).

The front at the western boundary of the Tsushima Current, and the shape of eddies generated off the mouth of the Chang River are clearly shown by the biband picture of R1/R3.

The relationship between the "pigment concentration (sum of chlorophyll and phaeopigments)" P′ (mg/cub. m, accumulated mean between 0 to 20 m) and radiance count is ;

$log\ P' = 2.479 - 6.539\ log\ (\text{R1}/\text{R3})$

and the correlation coefficient between log P and log (R1/R3) is −0.83 (Tab. 6—10, Fig. 13—14).

Comparison to the data obtained by R/V Yōkō-Maru (Fig. 16—27) shows the location of the front in the west of Kyushu seen in temperature, salinity, and pigment concentration well conforming with that seen in the biband picture. The water mass identification which has to do with fishing ground formation is difficult by means of surface temperature in summer in this area, while it can be done by means of the biband picture.

As Gordon et al. dealt both Reyleigh and aerosol scatterings uniform throughout the scene, the radiance count numbers of each band of all sea truth points were adjusted by each constant value for each band respectively, so as to increase the correlation between their ratio and the pigment index. This method was found, however, not very effective (Fig. 15). The value of both Reyleigh and aerosols' scattering was calculated after Gordon's method (Tab. 11—14). The value of e (λ, 670) which is pertaining to the optical depth was compared with that obtained by other authors in other areas (Tab. 15, 16).

Under present circumstance in which air-truth data are insufficient, the picture based on ratios R1/R3 of R1/SR is effective to eliminate the effect of the path radiance to some

extent and therefore applicable for the practical uses such as the estimation or chlorophyll distribution or water mass identification. Moreover, the gray pcale picture of biband can be used for practical uses instead of the false colour picture (Pl. 22).

For the precise quantitative analysis of chlorophyll estimation both sea and air thuth data are indispensable. For the practical view of fisheries, however, rapid processing of biband prcture can make a valuable contribution eventhough trere are only poor data sea and air truth.

Appendex. The geographical coordinates or anchor pixels of two scanning lines were discussed and it was shown that the scanning line can be expressed by means of a fifth power polynomial of the latitude when it is plotted on a rectangular coordinates.

References

Austin, R. W. (1982) : (Untitled), Attachment J, Minutes 18 th NET meeting, NET

El Sayed, S. Z. (1982) : CZCS algorithm summary, Attachment K-1, Minute 18 th NET meeting

Gordon, H. R. ; Clark, D. K. ; Muller, J. L. and Hovis, W. A. (1980) : Phyto-plankton pigment from the NIMBUS-7 Coastal Zone Colour Scanner, comparison with surface measurement. *Scıence*, **210**, 63-66.

Gordon, H. R. (1981) : (Untitlled), Attachment B., Minutes 15 th NET meeting.

Hovis, W. A. ; and Leung, K. C. (1977) : Remote sensing of ooean colour. *Optical Engeneerıng*, **16**-(2), 158-166.

Hulbert, E. O. (1943) : Propagation of radiance in a scattering and absorbing medium. *J. Opt. Soc. of America*, **33**, 52-45.

Inoue, N. (1981) : Hydrographic characteristics in the East China Sea, (in "The Biology of Gotō") published by the Biological Society of Nagasaki (in Jap.).

Kemmerer, A. J. and Butter, J. A. (1977) : Finding fish with satellites. *Marine Fish. Rev.* (**1230**), 15-19.

Ohwada, M. (1971) : Distribution of chlorophyll and phaeophytin in the Sea of Japan, *Ocean. Mag.* **23**-(1), 21-32.

Ramsey, R. (1968) : Study of remote sensing of ocean colour. Final Rep. Contract NASA 1658.

Sturm, B. (1981) : (Untitled), Appendix D. Minutes 15 th NET meeting.

Sturm, B, (1982) : Development in CZCS data evaluation at JRC Ispra during 1981 ; Attachment L, Minutes 18 th NET meeting.

Uno, S. (1978) : Report on the remote sensing study on red tide using aircraft, Vol. 1, Nansei Regional Fish. Res. Lab. and Asia Aeronautical Survey Co. Ltd. (in Jap.)

Uno, S. (1979) : ibid. Vol. 2.

Uno, S. (1980) : ibid. Vol. 3

Watanabe, K. (1977) : Artificial satellite data applicable to oceanographic research. *Kaiyo Kagaku* (*Marine Science Monthly*), Vol. **9**, (6), 34-44 (in Jap).

Wrigley, R. C. and Klooster, S. A. (1978) : Spectrometer measurement of water color in the Gulf of Mexico ; Minutes 9 th NET meeting.

Appendix : a consideration for gometric correction of CZCS data

(Shape of scanning line on the earth surfaee)

As was described in the text, every scanning line of CZCS has 78 anchor pixels of which latitude and longitude are shown. By using these data, the shape of the scanning line on the Earth was studied.

(1) Material used :

All data of latitude and longitude of anchor pixels on the line No. 1 and No. 2 of the Orbit #1998 (Off Baja California) were available by the preliminary exercise described in III—1 in the text.

(2) Plotting.

Fig. A 1 shows the plotted shape of the track of the scanning line No. 1 on the, rectangular coordinates ; the lattitude in the abscissa and the longitude as the ordinate, namely in somewhat different way from the actual geographic expression.

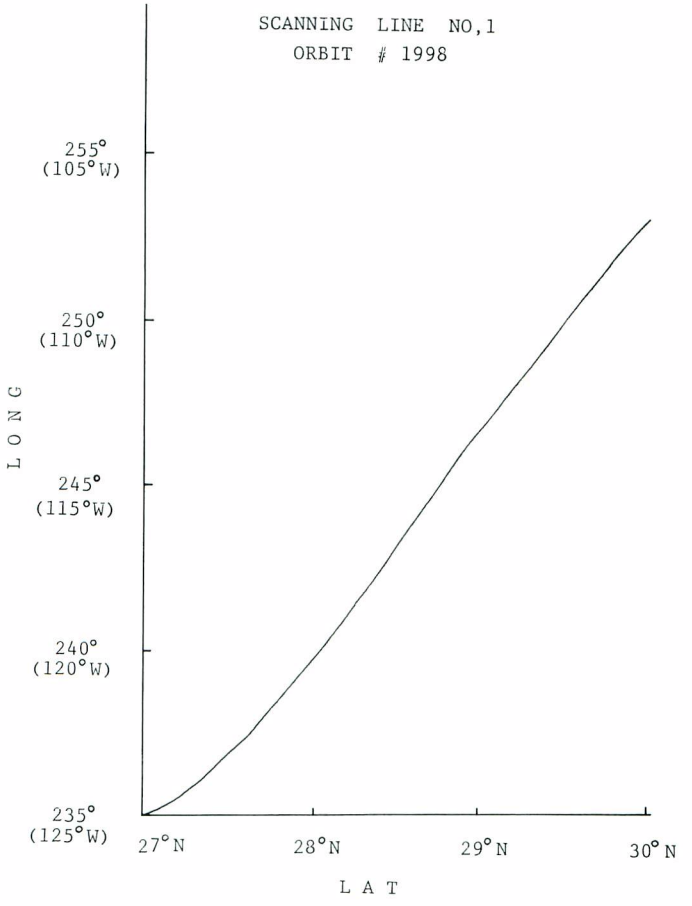

Fig. A 1 Plotted shape of the scanning line No. 1, CZCS Orbit 1998

(3) Empirical formula for the curve

It may be possible to solve the shape of the track of a scanning line on the earth analytically by means of the location and movement of the satellite on the orbit. Here, however, an empirical method was adopted to obtain the curve by using a high power series.

It was suggested from the elongated S shape of the graph of Fig. A 1 that the expression might have the power of the odd number order. Therefore the following expression were supposed ; namely putting the latitude as X and the longitude as Y ;

$$Y = A + B \cdot X$$
$$Y = A + B \cdot X + C \cdot X^2 + D \cdot X^3$$
$$Y = A + B \cdot X + C \cdot X^2 + D \cdot X^3 + E \cdot X^4 + F \cdot X^5$$
$$Y = A + B \cdot X + C \cdot X^2 + D \cdot X^3 + E \cdot X^4 + F \cdot X^5 + G \cdot X^6 + H \cdot X^7$$

and so on.

By comparing the computed value with the ovserved one, and obtaining the value of the mean square residuals, we can know which order of power is most adequate to adopt as the approximation.

For the computation 17 pixels were picked up from the 78 anchor pixels. As to the latitude and longitude, the origin point of the coordinates was shifted to the position of the Pixel No. 1. The Table A 1 shows the coordinates of the sempled pixels.

Table A 1. Coordinates. of anchor pixels of the scanning line No. 1 and No. 2, CZCS, Orbit #1998

No. of Pixel	Scan. Line No. 1		Scan. Line No. 2	
	Lat. X	Long. Y	Lat. X	Long. Y
1	0	0	0	0
91	0.217	1.199	0.217	1.196
166	0.375	2.077	0.374	2.077
256	0.542	3.028	0.542	3.029
366	0.723	4.075	0.723	4.075
496	0.913	5.193	0.912	5.193
666	1.133	6.523	1.133	6.524
886	1.391	8.124	1.391	8.124
1128	1.658	9.833	1.658	9.834
1343	1.898	11.421	1.898	11.422
1503	2.085	12.706	2.085	12.706
1628	2.242	13.81	2.242	13.812
1733	2.385	14.843	2.385	14.844
1818	2.511	15.770	2.511	15.771
1893	2.631	16.680	2.631	16.681
1968	2.765	17.716	2.765	17.717

There is substantially no difference in their coordinates of the two lines because

they are too close each other, Therefore the Scanning Line No. 1 was dealt alone.

The number of the order of power and the mean square residuals are shown below.

9 th	Power	MSR* =	0.00185
7 th	:	:	0.000947
5 th	:	:	0.000892
3 rd	:	:	0.0074

*mean square residual

Thus the fifth power was adopted for best fitting.

The coefficients of the empirical formula are ;

$$Y = A + B \cdot X + C \cdot X^2 + D \cdot X^3 + E \cdot X^4 + F \cdot X^5$$

$$A = 1.12358 \times 10^{-3}$$

$$B = 2.5505 \times 10^{-1}$$

$$C = 1,02029$$

$$D = 1.4675 \times 10^{-3}$$

$$E = -5.80116 \times 10^{-5}$$

$$F = 1.05997 \times 10^{-6}$$

The Fig. A 2 shows the comparison of the computed (line) and observed (circle) values.

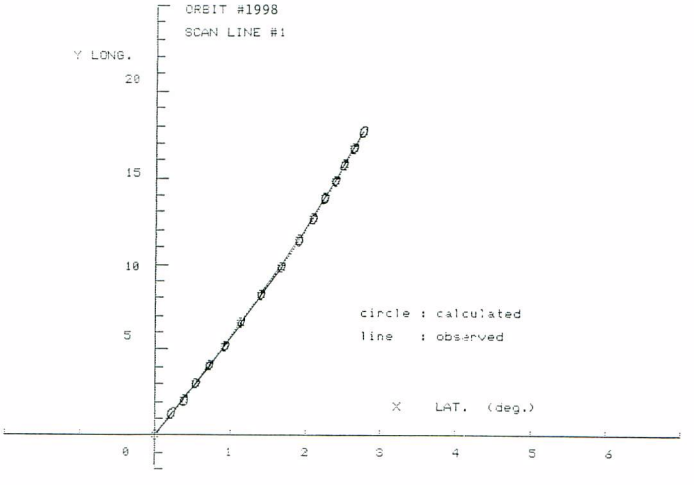

Fig. A 2 Comparison of computed and observed scanning ine No. 1 Orbit #1998

日本近海における NIMBUS-CZCS の画像解析

山中一郎・細村　宰・小笹悦二

摘　要

この報告は，非エネルギー分野における日米科学技術協力計画の１課題として，1979年に開始された人工衛星 NIMBUS-CZCS の画像解析結果について検討したものである。

研究に先だち，米国西岸のテープを用いて解析に必要なソフトウェアの開発，並びに画像製作を試みた。（P1. 1—4)。その結果，第１および第３の各バンドの比画像がクロロフィル量と関係深いことが示された。そこで1981年迄に米国から提供された合計15シーンの資料の中から，雲の状況にもとずいて２シーンを選び出して解析を行った。

(1) 軌道1297号（本州南方，1979年１月26日）：各バンドの画像，合成フォルスカラー，第１及び第３バンド比画像等を，前年に開発したソフトウェアを用いて製作した。（P１．６—12)。また，海面照合点付近の画素抽出，輝度統計量の計算等のソフトウェアを追加開発した。照合用資料は，やや遅れて実施された気象庁の観測結果を用いた。その結果，第６バンド（赤外線）画像は，黒潮の紀州沖大蛇行を明示し，これは船舶観測結果と合致していた（P１．10.Fig.６)。

照合資料と衛星資料との関係について種々の統計分析を行った（Tab.１—５．Fig.７—10)。照合点を中心とする画素クラスターの輝度分布のパターンにより，雲をある程度分離すると，水深０—10 m のクロロフィル量平均密度C（mg/cub. m）と第１及び第３バンドの最小輝度カウント数の比（min.R１/min.R３）との間には，

$$\log C = -4.54 \log (\text{min.R}1/\text{min.R}3) + 1.019 \quad (r = -0.82)$$

という関係が認められ，また，各バンドの輝度値（最小）をR１とし，Ri = Ri/∑RSi としてRSiとCとの相関係数を求めると，第１及び第３バンドでこの値は高くかつ符号が逆であり，一方第２バンドでは相関が低く，いわゆるヒンジポイントである事が示された（Tab.５)。

(2) 軌道8774号（九州西方，1980年７月20日：……前の例と同様の写真（P１．13—19，21）のほか，図上に緯経度線を挿入し，メルカトール図に転換するためのソフトを新に開発し，これを用いた解析を行った（P１．20，22，23)。

R１とR３との比画像により，東シナ海中央部，対馬暖流外縁の潮境，長江河口沖合の河川水と外洋水との間の渦動の形状が明示された。そこで，同時期の陽光丸による観測結果をもとに，クロロフィルａ量とフェオ色素との和を"色素密度"（P' mg/cub. m. 但し水深０—20 m の積算平均値）で示すと，次式が得られた（Tab.６—10，Fig.13—14)。

$$\log P' = -2.479 - 6.539 \log (R1/R3) \quad (r = -0.83)$$

（Rはこの場合最小輝度数）

水温，塩分，色素量等の分布にみられる九州西方の前線の位置は比画像にみられるものとほぼ一致しており，また，夏季のまき網漁場と関係の深い水塊の判別が，表面水温では困難であるにも拘らず，比画像では可能であると考えられた（Fig.16—27)。

大気補正について，Gordon 等（1981）の方法では，レーリー及びエアロゾルの両散乱量が共に全画面で一様であるとして扱っていることから，全照合点について各輝度値から夫々一定値を補正し，その比と，夫々の色素指数の対数との間の相関係数の値を高める事を試みたが，あまり大きな効果はなかった（Fig.15)。また両散乱量を Gordon 法を用いて求め（Tab.11—14)，各波長帯の光学深度に関する e（λ, 670）の値を他の著者によるものと比較した（Tab.15—16)。その結果，大気補正に用いる実測照合値が不備である現在，比画像，またはRi/∑Ri による方法がパスラデアンスを除き，クロロフィル量分布推定や水塊判別の様な実用目的には利用で

き，また比画像はフォルスカラーに代りグレイスケールでも実用性のあること（pl. 22）が示された。

クロロフィル量の推定には，海面及び大気の照合資料が必要である。しかし，水塊判別等の漁業上の実用性からみれば，完全な照合資料がなくても，迅速に比画像を作成する事の方が効果的であると考えられる。

（補遺）：幾何補正についての一考察（地表上の走査線の形状）

走査線上のアンカーピクセルの緯経度について検討し，緯経度を直角座標で示した場合，走査線は緯度の5次式で近似されることを示した。

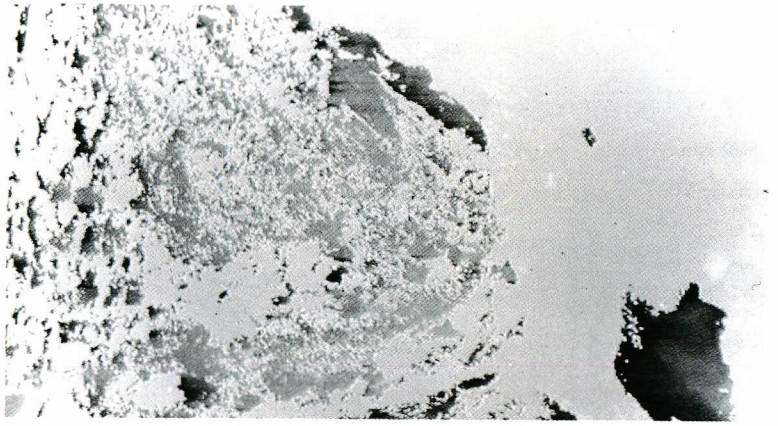

Plate 1. Ratio image of R1/(R1+R2+R3+R4), Orbit #1998 (off Baja California)

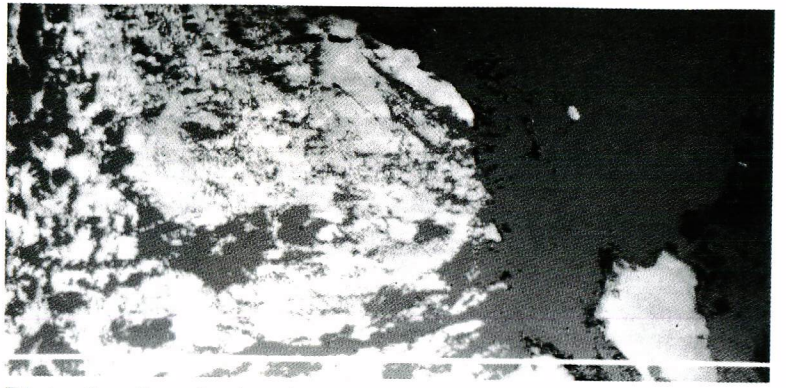

Plate 3. ditto: R1/R2 (in monochromatic)

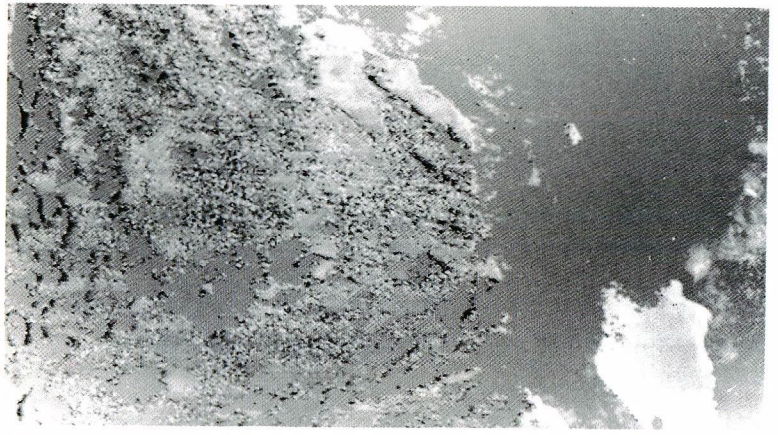

Plate 2. ditto: R3/(R1+R2+R3+R4)

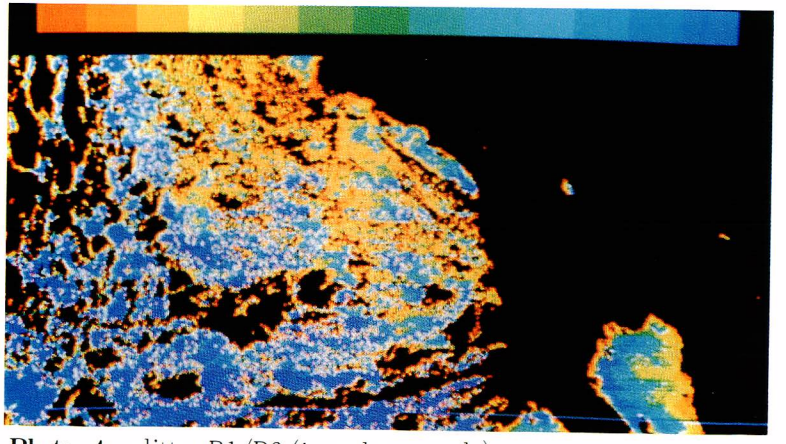

Plate 4. ditto: R1/R2 (in colour scale)

Plate 5. Monoband image of Band 1, Orbit #1297 (Off South Honshu) JAN. 26, 1979

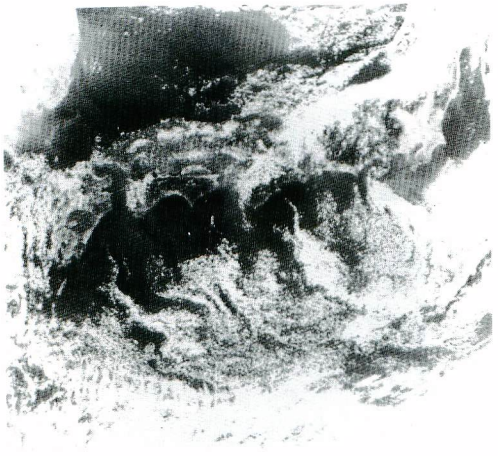

Plate 6. ditto: Band 2

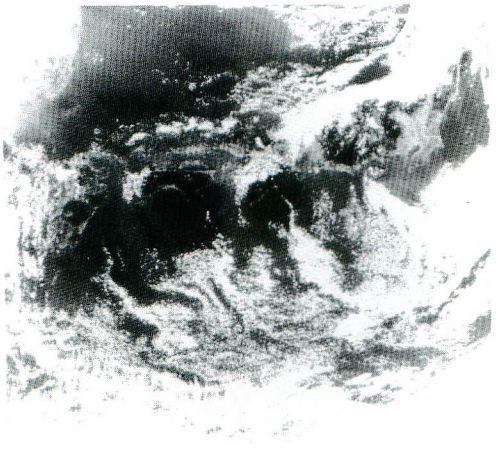

Plate 7. ditto: Band 3

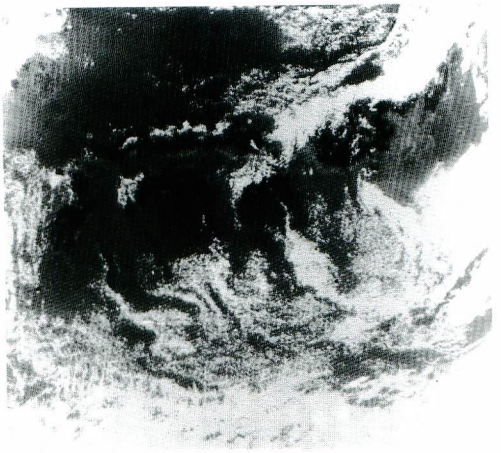

Plate 8. ditto: Band 4

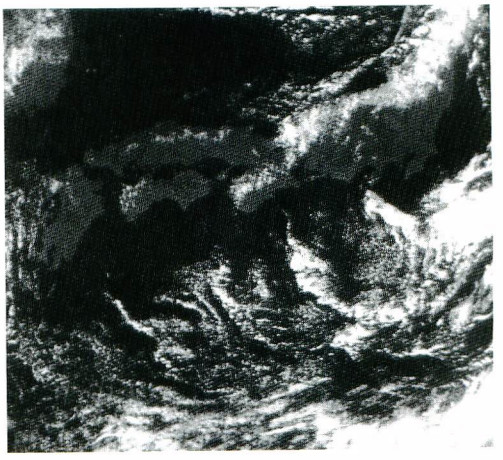

Plate 9. ditto: Band 5

Plate 10. ditto. Band 6

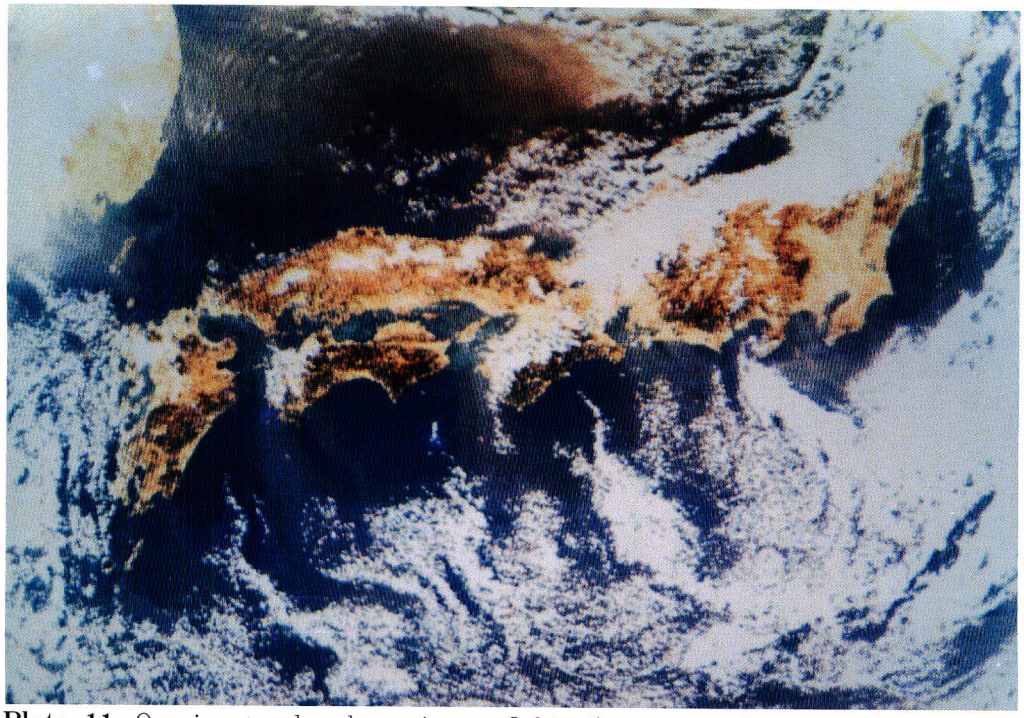

Plate 11. Quasi natural colour picture, Orbit #1297 , 1 ; B, 3 ; G, 5 ; R

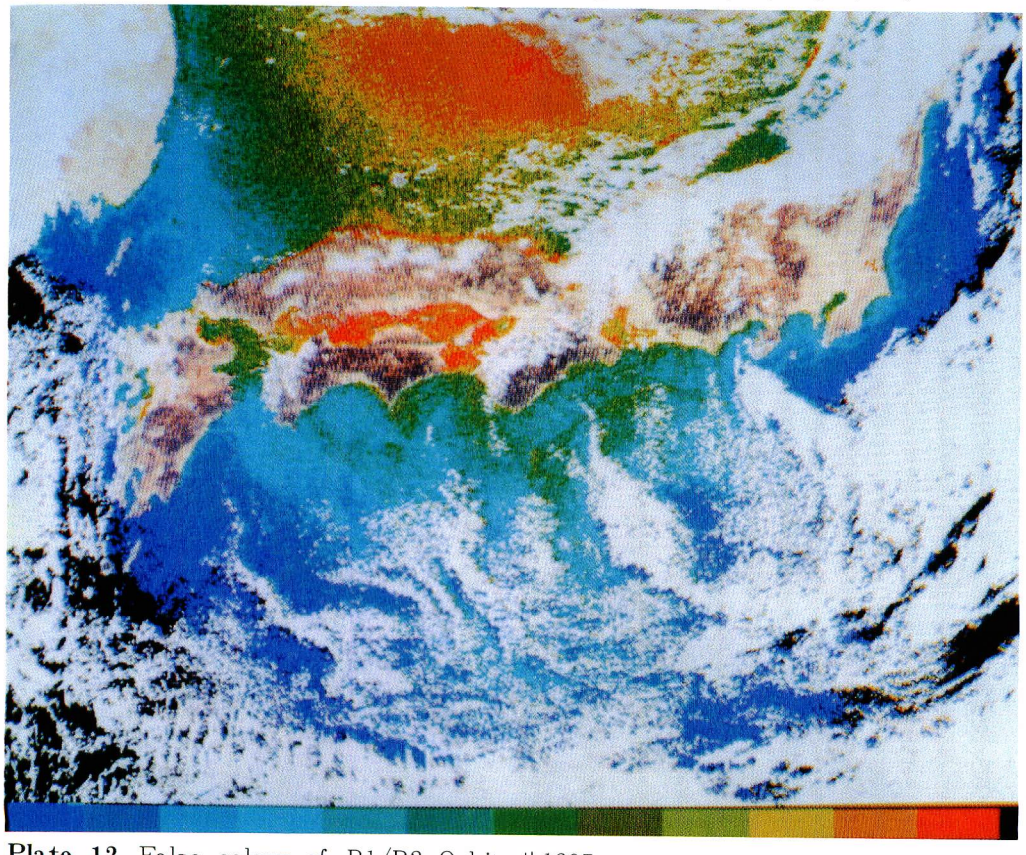

Plate 12. False colour of R1/R2, Orbit #1297

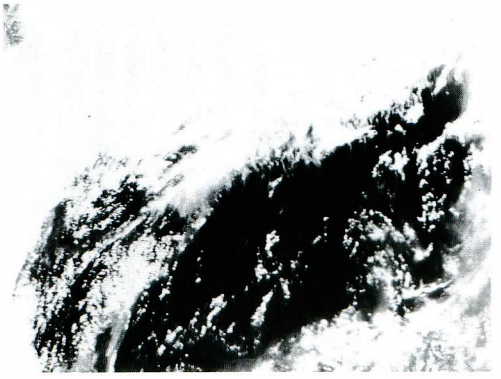

Plate 13. Monoband image of Band 1, Orbit #8774 (East China Sea)

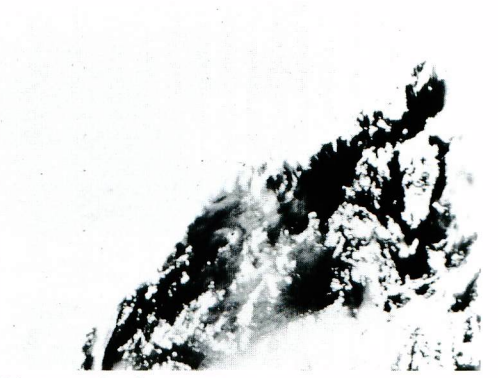

Plate 16. ditto: Band 4

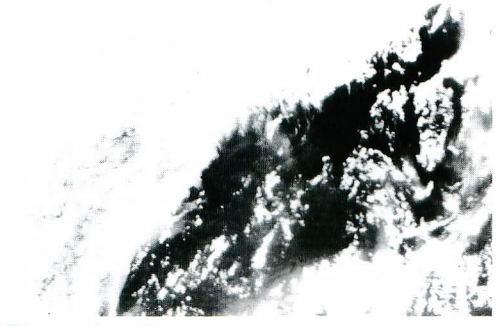

Plate 14. ditto: Band 2

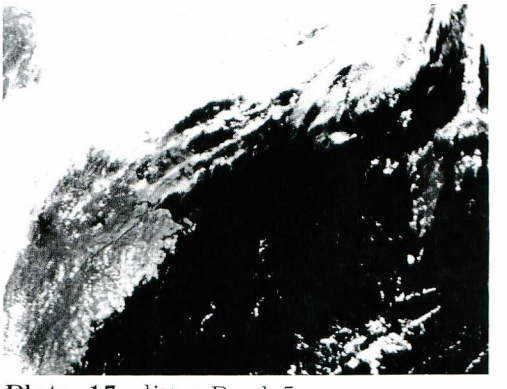

Plate 17. ditto: Band 5

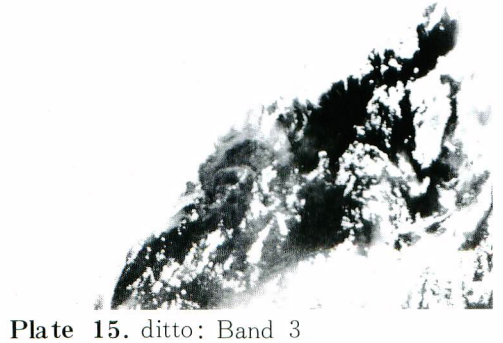

Plate 15. ditto: Band 3

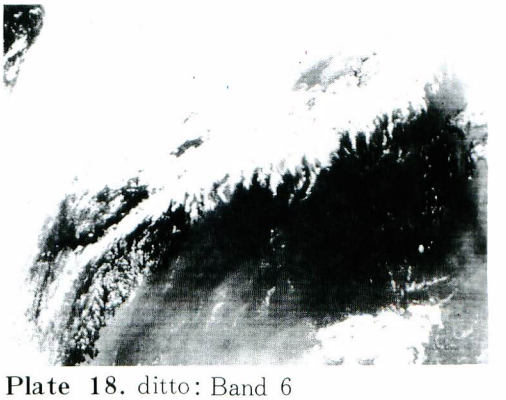

Plate 18. ditto: Band 6

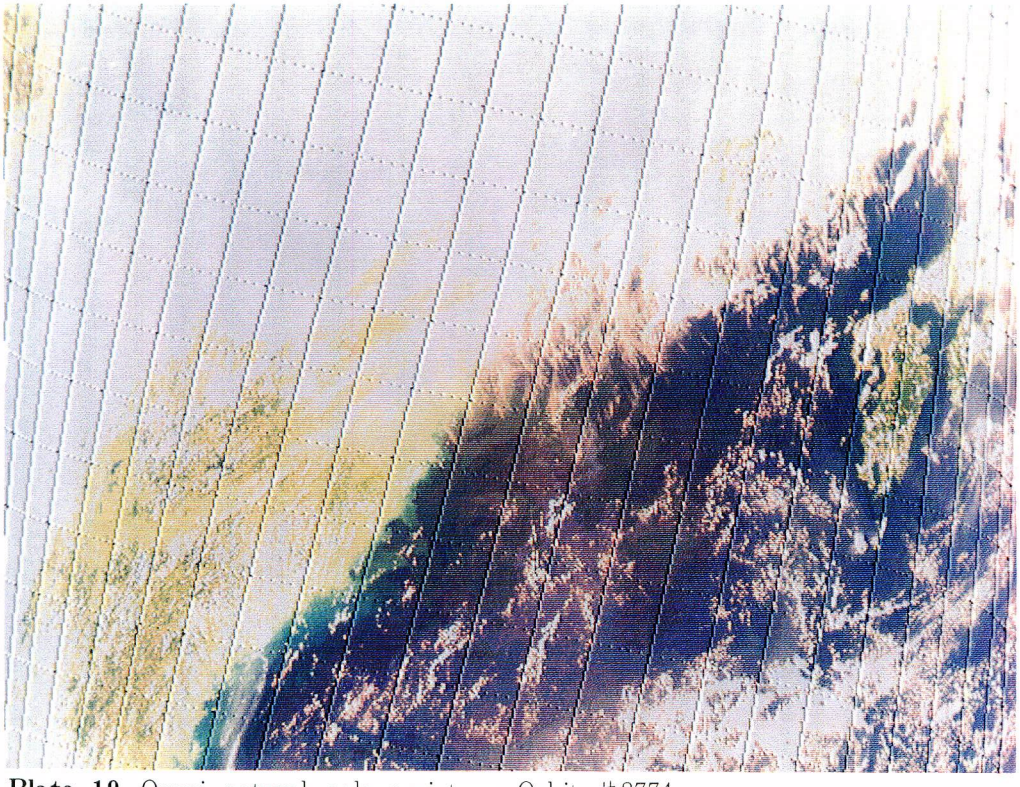

Plate 19. Quasi natural colour picture, Orbit #8774

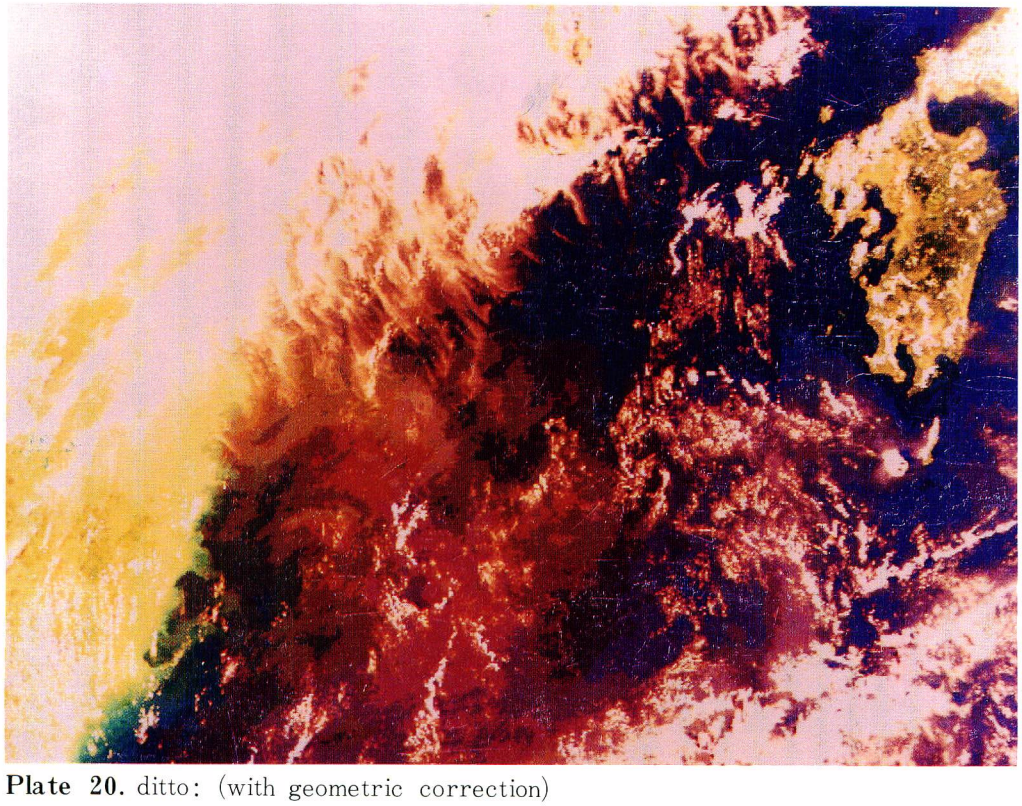

Plate 20. ditto: (with geometric correction)

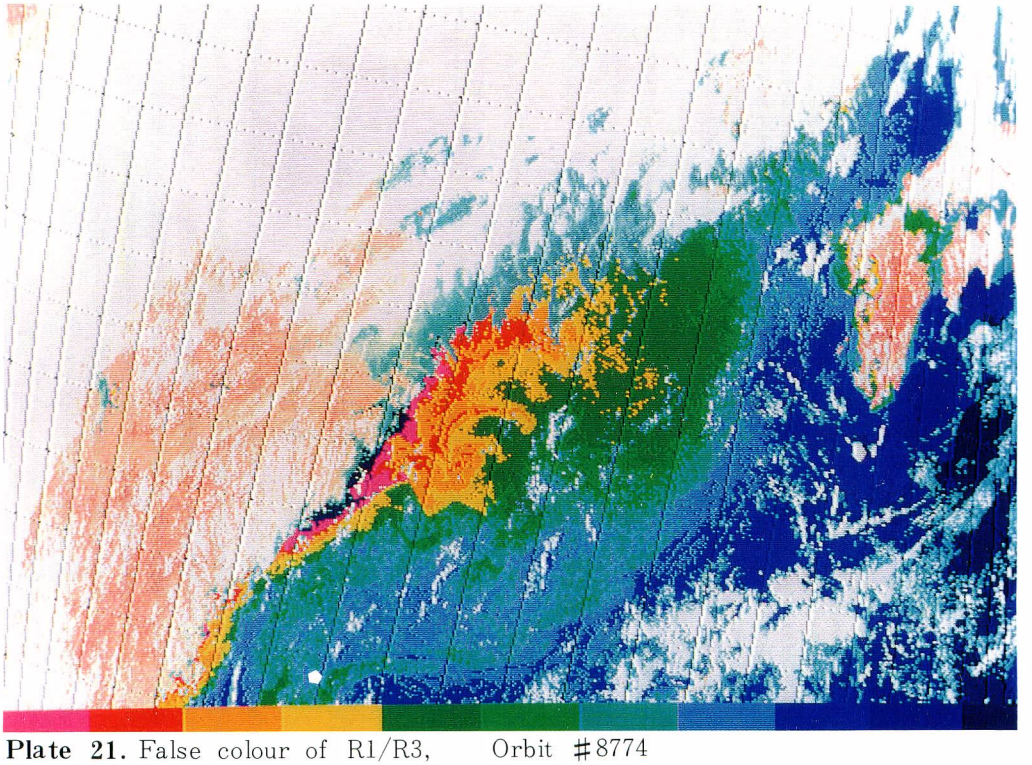

Plate 21. False colour of R1/R3, Orbit #8774

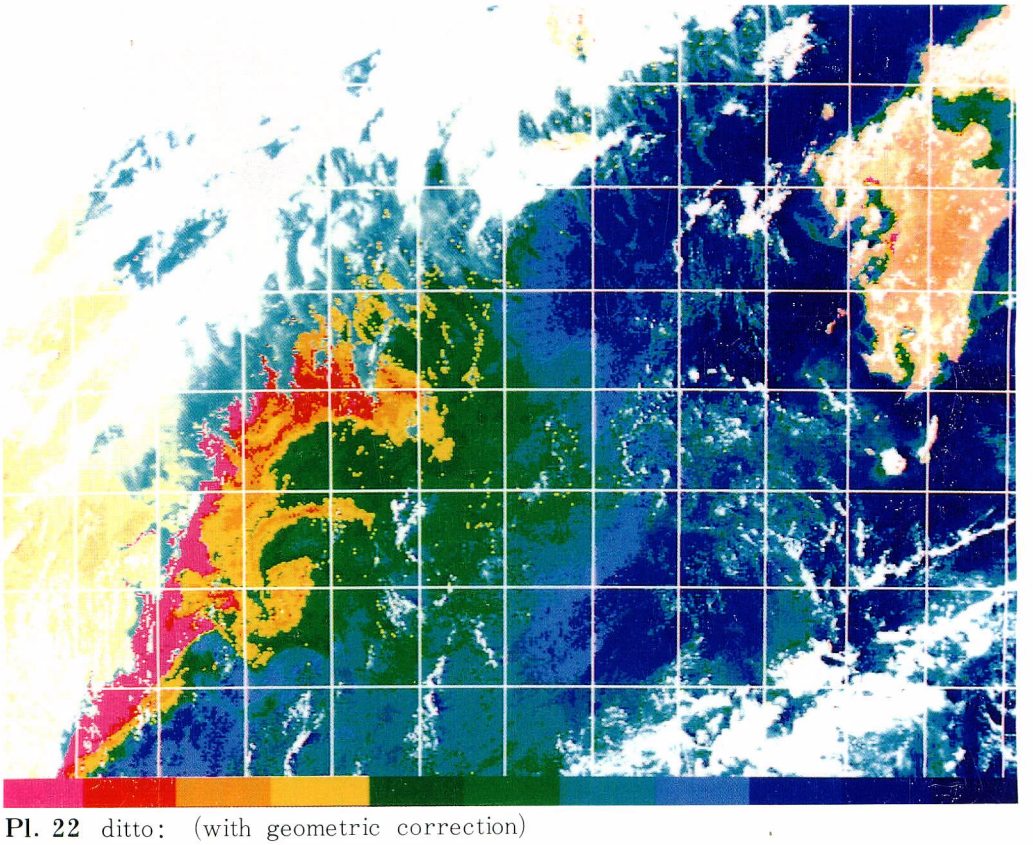

Pl. 22 ditto: (with geometric correction)